MARTIN MARIETTA ENERGY SYSTEMS LIBRARIES

3 4456 0313499

ORNL/CON-274

ornl

OAK RIDGE
NATIONAL
LABORATORY

MARTIN MARIETTA

Model for Roof Thermal Performance

K. E. Wilkes

OAK RIDGE NATIONAL LABORATORY
CENTRAL RESEARCH LIBRARY
CIRCULATION SECTION
4500N ROOM 175
LIBRARY LOAN COPY
DO NOT TRANSFER TO ANOTHER PERSON
If you wish someone else to see this report, send in name with report and the library will arrange a loan.

OPERATED BY
MARTIN MARIETTA ENERGY SYSTEMS, INC.
FOR THE UNITED STATES
DEPARTMENT OF ENERGY

This report has been reproduced directly from the best available copy.

Available to DOE and DOE contractors from the Office of Scientific and Technical Information, P.O. Box 62, Oak Ridge, TN 37831; prices available from (615) 576-8401, FTS 626-8401.

Available to the public from the National Technical Information Service, U.S. Department of Commerce, 5285 Port Royal Rd., Springfield, VA 22161.
NTIS price codes—Printed Copy: A05 Microfiche A01

This report was prepared as an account of work sponsored by an agency of the United States Government. Neither the United States Government nor any agency thereof, nor any of their employees, makes any warranty, express or implied, or assumes any legal liability or responsibility for the accuracy, completeness, or usefulness of any information, apparatus, product, or process disclosed, or represents that its use would not infringe privately owned rights. Reference herein to any specific commercial product, process, or service by trade name, trademark, manufacturer, or otherwise, does not necessarily constitute or imply its endorsement, recommendation, or favoring by the United States Government or any agency thereof. The views and opinions of authors expressed herein do not necessarily state or reflect those of the United States Government or any agency thereof.

ORNL/CON-274

Energy Division

MODEL FOR ROOF THERMAL PERFORMANCE

K. E. Wilkes

Date Published - July 1989

Building Thermal Envelope Systems and Materials Program

Prepared for the
U.S. Department of Energy
Office of Buildings and Community Systems

Prepared by the
OAK RIDGE NATIONAL LABORATORY
Oak Ridge, Tennessee 37831
operated by
MARTIN MARIETTA ENERGY SYSTEMS, INC.
for the
U.S. DEPARTMENT OF ENERGY
Under Contract No. DE-AC05-84OR21400

MARTIN MARIETTA ENERGY SYSTEMS LIBRARIES

3 4456 0313499 9

CONTENTS

LIST OF FIGURES v

LIST OF TABLES ix

ABSTRACT xi

EXECUTIVE SUMMARY xiii

NOMENCLATURE xvii

1. INTRODUCTION 1

2. DEVELOPMENT OF THERMAL MODEL 3

2.1 MATHEMATICAL MODEL 3
2.2 COMPUTER IMPLEMENTATION 14
2.3 INSTRUCTIONS FOR RUNNING PROGRAM 20
2.4 PLANS FOR FURTHER DEVELOPMENT 21

3. COMPARISON OF MODEL WITH EXPERIMENTS 23

3.1 EXPERIMENTAL SETUP 23
3.2 EXPERIMENTAL RESULTS 25
3.3 MODEL VERIFICATION 28

4. SUMMARY AND CONCLUSIONS 47

REFERENCES 49

APPENDIX A, STAR COMPUTER PROGRAM 51

APPENDIX B, BASIC INPUT FOR STAR PROGRAM (INTERACTIVE) 65

APPENDIX C, BASIC INPUT FOR STAR PROGRAM (EXTERNAL FILE) . . . 73

LIST OF FIGURES

2.1 Finite Difference Grid. 5

2.2 Node Spacings for Effective Thermal Conductivity. 5

2.3 Flow Chart for STAR Computer Program. 15

3.1 Cross Section of Experimental Roof Panels 24

3.2 Measured Outdoor Temperatures 24

3.3 Measured Solar Radiation. 26

3.4 Measured Incident Infrared Radiation. 26

3.5 Measured Membrane Temperatures. 27

3.6 Measured Roof Heat Fluxes 27

3.7 Comparison of Predicted and Measured Roof Heat Fluxes for Bare Roof in Cool Weather With Given Boundary Temperatures at Top of Membrane, Using Constant Thermal Properties. 29

3.8 Comparison of Predicted and Measured Roof Heat Fluxes for Bare Roof in Cool Weather With Given Boundary Temperatures at Top of Insulation, Using Constant Thermal Properties. 31

3.9 Comparison of Predicted and Measured Roof Heat Fluxes for Bare Roof in Cool Weather With Given Boundary Temperatures at Top of Insulation, Using Temperature-Dependent Insulation Thermal Conductivity 31

3.10 Comparison of Predicted and Measured Roof Heat Fluxes for Bare Roof in Warm Weather With Given Boundary Temperatures at Top of Membrane, Using Constant Thermal Properties. 32

3.11 Comparison of Predicted and Measured Roof Heat Fluxes for Bare Roof in Warm Weather With Given Boundary Temperatures at Top of Insulation, Using Temperature-Dependent Insulation Thermal Conductivity 32

3.12 Comparison of Predicted and Measured Roof Heat Fluxes for Paver Roof in Cool Weather With Given Boundary Temperatures at Top of Paver, Using Temperature-Dependent Insulation Thermal Conductivity 34

3.13 Comparison of Predicted and Measured Roof Heat Fluxes for Paver Roof in Warm Weather With Given Boundary Temperatures at Top of Paver, Using Temperature-Dependent Insulation Thermal Conductivity 34

3.14 Comparison of Predicted and Measured Membrane Temperatures for Bare Roof in Cool Weather With Weather Boundary Conditions, Using Temperature-Dependent Insulation Thermal Conductivity 35

3.15 Comparison of Predicted and Measured Roof Heat Fluxes for Bare Roof in Cool Weather With Weather Boundary Conditions, Using Temperature-Dependent Insulation Thermal Conductivity. 35

3.16 Comparison of Predicted and Measured Roof Heat Fluxes for Bare Roof in Cool Weather With Weather Boundary Conditions, Using Temperature-Dependent Insulation Thermal Conductivity and Modified Infrared Radiation. . . 37

3.17 Comparison of Predicted and Measured Roof Heat Fluxes for Bare Roof in Cool Weather With Weather Boundary Conditions, Using Temperature-Dependent Insulation Thermal Conductivity and Solar Absorptance of 0.9 37

3.18 Comparison of Predicted and Measured Roof Heat Fluxes for Bare Roof in Cool Weather With Weather Boundary Conditions, Using Temperature-Dependent Insulation Thermal Conductivity and Convection Coefficient 20 Percent Lower Than Normal. 39

3.19 Comparison of Predicted and Measured Membrane Temperatures for Paver Roof in Cool Weather With Weather Boundary Conditions, Using Temperature-Dependent Insulation Thermal Conductivity. 39

3.20 Comparison of Predicted and Measured Roof Heat Fluxes for Paver Roof in Cool Weather With Weather Boundary Conditions, Using Temperature-Dependent Insulation Thermal Conductivity. 40

3.21 Comparison of Predicted and Measured Roof Heat Fluxes for Paver Roof in Cool Weather With Weather Boundary Conditions, Using Temperature-Dependent Insulation Thermal Conductivity and Modified Infrared Radiation. . . 40

3.22 Comparison of Predicted and Measured Membrane Temperatures for Bare Roof in Warm Weather With Weather Boundary Conditions, Using Temperature-Dependent Insulation Thermal Conductivity. 42

3.23 Comparison of Predicted and Measured Roof Heat Fluxes for Bare Roof in Warm Weather With Weather Boundary Conditions, Using Temperature-Dependent Insulation Thermal Conductivity. 42

3.24 Comparison of Predicted and Measured Roof Heat Fluxes for Bare Roof in Warm Weather With Weather Boundary Conditions, Using Temperature-Dependent Insulation Thermal Conductivity, Modified Infrared Radiation, and Solar Absorptance of 0.7. 43

3.25 Comparison of Predicted and Measured Membrane Temperatures for Paver Roof in Warm Weather With Weather Boundary Conditions, Using Temperature-Dependent Insulation Thermal Conductivity. 43

3.26 Comparison of Predicted and Measured Roof Heat Fluxes for Paver Roof in Warm Weather With Weather Boundary Conditions, Using Temperature-Dependent Insulation Thermal Conductivity. 44

3.27 Comparison of Predicted and Measured Roof Heat Fluxes for Paver Roof in Warm Weather With Weather Boundary Conditions, Using Temperature-Dependent Insulation Thermal Conductivity, Modified Infrared Radiation and Solar Absorptance of 0.7. 44

LIST OF TABLES

2.1 Correlations for Convection Coefficients. 11

2.2 Data Entered by Keyboard or From External File. 17

3.1 Material Properties and Geometric Values Used in Models . 29

3.2 Comparison of Predicted and Measured Peak Membrane Temperatures and Weekly Heat Flows. 45

ABSTRACT

This report describes a model that has been developed for predicting heat flows and temperatures within roof systems. The model is called STAR (for Simplified Transient Analysis of Roofs). It applies to transient one-dimensional conduction in multilayer roof systems and is fully coupled to ambient weather conditions. It has been implemented on a personal computer and has been designed to be easy to use for a variety of problems. The report gives details of the mathematical model and a verification of the model by comparing its predictions with existing experimental data.

EXECUTIVE SUMMARY

Models play an important role in the operation of the Roof Research Center. They increase the efficiency of costly experimentation by guiding the placement of sensors, identifying critical experiments, and extrapolating the results of experimental data to conditions other than those which were tested. Models are essential to developing an understanding of the complex interactions of the thermal, moisture, and mechanical behaviors of roofs. Finally, models provide tools to aid the design of more energy efficient and durable roofs.

The objective of this project was to develop a flexible easy-to-use computer model for transient one-dimensional heat transfer in multilayer roof systems with full coupling to ambient conditions. The model was to take into account temperature dependent thermal properties and was to utilize a numerically stable solution method that does not require exceedingly small time steps and consequent long computational times.

The computer model that was developed is named STAR (for Simplified Transient Analysis of Roofs). It is a transient one-dimensional finite difference model for heat conduction. The model can simulate heat flow in multilayer roof systems with materials that have thermal conductivities and specific heats that vary with temperature. Two types of boundary conditions are handled by the model. With the first type, the boundary temperatures are specified. This is useful for analyzing experimental data where the surface temperature has been measured. With the second type, conduction in the roof system is coupled with convection and radiation heat exchanges with the outdoor or indoor environment. The outdoor environment includes the effects of solar radiation, infrared radiation, outdoor temperature, wind speed, and relative humidity.

Several methods of solution of the transient equations are included in the model. These are the classical explicit, fully implicit, and Crank-Nicolson methods. The classical explicit method has the disadvantage that if the time step for the solution is not chosen to be small enough, the numerical solution may become unstable and physically unrealistic solutions may be generated. The fully implicit method does not have this drawback; it is numerically stable for any size of time step. However, the time step must be chosen to be small enough to track the changes in temperatures and heat flows in the system being modeled.

The model has been implemented on an IBM AT personal computer. Two methods of entering basic input data have been provided. With one method, basic input data are entered interactively on the keyboard with prompts being displayed on the monitor. With the other method, the same input data are read from an external file. The model allows choices for the type of boundary conditions, convection coefficients, and whether to include latent heat effects due to moisture condensation or evaporation at the exterior surface. The model calculates hourly values of temperatures and heat fluxes at the external surfaces of the roof and at all interfaces between material layers. The model also calculates the amount of moisture accumulated on the exterior surface.

The model has been verified by comparing its predictions with field data measured on roof sections at the Roof Thermal Research Apparatus. The experimental data were obtained during a cool week in January and February and during a warm week in May. The data were obtained on a roof section insulated with fiberglass insulation and covered with a modified bitumen membrane and on a similar roof section with a layer of concrete pavers added on top.

From visual inspections of plots of membrane temperature and roof heat flow, the model is judged to work very well, especially when the boundary temperatures are known. The models capture the most important

features of the diurnal cycles, the trends in weather during the weekly periods, and major differences between the weather conditions in the two weeks.

It has been demonstrated that the use of a temperature dependent thermal conductivity for the fiberglass insulation results in improved predictions. It appears that significant improvements can be obtained with refinements in the values for incident infrared radiation, solar absorptance, and also possibly in the values that are used for the convection heat transfer coefficients.

While the STAR model is useful in its present form, it will continue to be developed. In its present form, the user must supply values for the material properties. It is planned to build a library of material properties into the program from which the user may select values. It is also planned to add other phenomena to the model. These will include the movement of moisture due to diffusion and convection. This will allow predictions of condensation, evaporation, freezing, and thawing through the thickness of the roof system. The model will also be coupled with other models for determining induced mechanical strains and stresses in the roof system.

NOMENCLATURE

C_p	specific heat
D	coefficient for diffusion of water vapor through air
Gr	Grashof number
L	characteristic length
Nu	Nusselt number
Pr	Prandtl number
Q	heat flow
Ra	Rayleigh number
Re	Reynolds number
T	temperature
V	air velocity
W	humidity ratio
f	weighting factor for transient solution technique
g	acceleration of gravity
h	convection heat transfer coefficient, or, with subscript m, convection mass transfer coefficient
k	thermal conductivity
$\dot{m}$	mass transfer rate
t	time
x	distance
α	solar absorptance, or thermal diffusivity
β	volume coefficient of thermal expansion of air
ϵ	infrared emittance
φ	tilt angle of roof
ρ	density
σ	Stefan-Boltzmann constant
ν	kinematic viscosity of air
ΔT	temperature difference
Δt	time difference between steps
Δx	width of control volume
δx	distance between nodes

Superscripts

0	denotes beginning of time step
1	denotes end of time step

Subscripts

E	pertains to node E
P	pertains to node P
W	pertains to node W
c	pertains to convection heat transfer
e	pertains to control volume face between nodes P and E
v	pertains to vaporization of water
w	pertains to control volume face between nodes P and W
s	pertains to surface of roof
air	pertains to ambient air
cond	pertains to conduction heat transfer

infrared	pertains to incident infrared radiation
latent	pertains to latent heat of vaporization
solar	pertains to solar radiation
surr	pertains to surroundings

1. INTRODUCTION

Models play an important role in the operation of the Roof Research Center. They increase the efficiency of costly experimentation by guiding the placement of sensors, identifying critical experiments, and extrapolating the results of experimental data to conditions other than those which were tested. Models are essential to developing an understanding of the complex interactions of the thermal, moisture, and mechanical behaviors of roofs. Finally, models provide tools to aid the design of more energy efficient and durable roofs.

A model that is already in use at the Roof Research Center is called PROPOR (for Properties, Oak Ridge).[1] This model is used for parameter estimation.[2] With this model, the known quantities are temperatures and heat fluxes at various points in the system. Using these as inputs, the model estimates values for the thermal conductivity and heat capacity.

This report describes a new model that is complementary to the PROPOR model. The new model is called STAR (for Simplified Transient Analysis of Roofs). It has been developed for predicting heat flows and temperatures within roof systems where the thermal properties are assumed to be known. It applies to transient one-dimensional heat transfer in multilayer roof systems and is fully coupled to ambient weather conditions. The model takes into account temperature dependent thermal properties. It utilizes a numerically stable solution method that does not require exceedingly small time steps and consequent long computational times. It has been implemented on a personal computer and has been designed to be easy to use for a variety of problems. This report gives details of the mathematical model and a verification of the model by comparing its predictions with existing experimental data.

2. DEVELOPMENT OF THERMAL MODEL

This section gives details of the mathematical model, numerical procedures, and computer implementation. It also outlines plans for further development of the model.

2.1 MATHEMATICAL MODEL

At its present stage of development, the STAR model consists of a numerical analysis of the one-dimensional transient heat conduction equation with appropriate boundary conditions at the two surfaces. In one dimension, the heat conduction equation is given by

$$\rho \, C_p \frac{\partial T}{\partial t} = \frac{\partial}{\partial x} \left(k \frac{\partial T}{\partial x} \right) \tag{1}$$

where

T = temperature

t = time

x = distance

k = thermal conductivity

ρ = density

C_p = specific heat

Except for very simple systems, exact analytical solutions of Equation 1 are very difficult to obtain. When the system consists of several layers of different materials, the thermal properties vary with temperature, and the boundary conditions consist of complicated coupling to ambient weather conditions, an approximate solution method is required. The finite difference solution method was chosen for this model for heat transfer in roofs where all the above conditions exist. With this method, the region of interest is broken into a grid of nodes

as shown in Fig. 2.1, at which temperatures are calculated. The representative node at point P has neighboring points to the east and west that are denoted by E and W. The point P is considered to be at the center of a control volume of width Δx. Although Fig. 2.1 shows the three nodes to be equally spaced, this is not a requirement of the method. The faces of the control volume around P are denoted by "e" and "w". As shown by Patankar[3], Equation 1 may be integrated over small increments of space and time to obtain the following discretized heat balance equation for node P:

$$\rho\, C_p \frac{\Delta x}{\Delta t} (T_P^1 - T_P^0) =$$

$$f \left[\frac{k_e\,(T_E^1 - T_P^1)}{(\delta x)_e} - \frac{k_w\,(T_P^1 - T_W^1)}{(\delta x)_w} \right]$$

$$+ (1 - f) \left[\frac{k_e\,(T_E^0 - T_P^0)}{(\delta x)_e} - \frac{k_w\,(T_P^0 - T_W^0)}{(\delta x)_w} \right] \qquad (2)$$

where

T_P = temperature at node P

T_E = temperature at node E

T_W = temperature at node W

Δx = width of control volume around node P

Δt = time difference between steps

ρ = density of the material at node P

C_P = specific heat of the material at node P

k_e = effective thermal conductivity between nodes P and E

k_w = effective thermal conductivity between nodes P and W

$(\delta x)_e$ = distance between nodes P and E

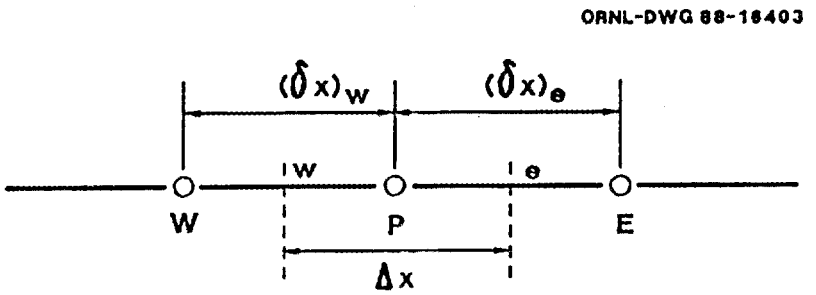

Fig. 2.1. Finite difference grid.

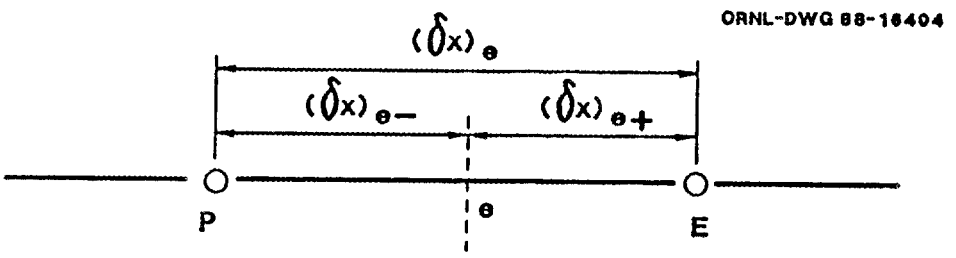

Fig. 2.2. Node spacings for effective thermal conductivity.

$(\delta x)_w$ = distance between nodes P and W

Superscript 0 denotes beginning of time step

Superscript 1 denotes end of time step

The power of the finite difference method is that it has transformed the partial differential equation in Equation 1 to a set of algebraic equations, one for each node. The left hand side of Equation 2 represents the change in energy stored within the control volume as the control volume temperature changes from Tp^0 at the beginning of the time step to Tp^1 at the end of the time step. The right hand side represents the net heat conducted into the control volume from the neighboring nodes. The quantity in the first brackets represents the heat conduction based on the temperatures at the end of the time step, while the quantity in the second brackets represents the heat conduction based on the temperatures at the beginning of the time step. The quantity "f" is a weighting factor which may be chosen between 0 and 1.

The choice of a value for f has a large influence on the ability to obtain physically realistic solutions. If f were chosen to be 0, the quantity in the first brackets on the right hand side of Equation 2 would not be involved. If all the temperatures were known at the beginning of the time step, then temperatures at the end of the time step could be calculated directly. This procedure is known as the classical explicit method. While this is a very simple method to implement, it has the pitfall that if the time step is not chosen to be small enough, the calculations can diverge and physically unrealistic solutions will be obtained. In order to avoid this catastrophe, the following stability criterion must be satisfied:

$$\Delta t < \rho Cp \, (\Delta x)^2/2k \qquad (3)$$

If small control volumes are needed to represent accurately the system being modeled, then correspondingly small time steps will be needed.

Thus, with the explicit method, a tradeoff must be made between accuracy of the solution and computational time.

When f is chosen to be 1, the second bracket on the right hand side is not involved. The temperature at node P at the beginning of the time step will be known, but all the other temperatures in the equation will be unknown. The set of equations for all the nodes will then have to be solved simultaneously. Because of this, the method with f equal to 1 is known as the fully implicit method. With the fully implicit method, no numerical stability problems are encountered no matter how large the time step is chosen. However, the time step would still have to be chosen to be compatible with the time scale of the problem being solved to obtain an accurate solution.

Between these two extremes is the choice of f equal to 0.5, where the terms in both brackets are weighted equally. This method is known as the Crank-Nicolson method. For small time steps, it provides the most accurate solutions. However, if the time steps are too large, the method can produce physically unrealistic oscillatory solutions.

All three solution methods have been incorporated in the STAR model. However, to avoid the possibility of physically unrealistic solutions, the fully implicit method is recommended.

Equation 2 shows thermal conductivities evaluated at the control volume faces. Within the model, each node has a thermal conductivity assigned to it. In this way, the thermal conductivity may vary from one node to another to allow different nodes to represent different materials, or to allow the thermal conductivity to vary with temperature. The effective thermal conductivities at control volume faces are determined by a series arrangement of the thermal resistances between two nodes as shown in Fig. 2.2. This results in the following equation for the effective conductivity:

$$k_e = \left[\frac{1 - f_e}{k_P} + \frac{f_e}{k_E} \right]^{-1} \tag{4}$$

where

$$f_e = \frac{(\delta x)_{e+}}{(\delta x)_e} \tag{5}$$

k_P = thermal conductivity of material at point P

k_E = thermal conductivity of material at point E

The STAR model allows two types of boundary conditions. One type is the specification of the boundary temperature. This is useful for analyzing experimental data. The second type utilizes the weather and interior room conditions to drive the thermal model. The exterior boundary condition consists of the following heat balance:

$$\alpha Q_{solar} + \epsilon Q_{infrared} + h\,(T_{air} - T_s) - \epsilon\sigma T_s^4 + Q_{latent} + Q_{cond} = 0 \tag{6}$$

The terms in this equation represent absorbed solar radiation, absorbed incident infrared radiation, convection from the air to the surface, radiation emitted by the surface, heat delivered to the surface by condensation of moisture (or removed by evaporation), and the heat conducted toward the surface from within the roof system. The quantities α and ϵ are the solar absorptance and infrared emittance of the surface. The surface is assumed to be gray in the infrared region, so that the infrared absorptance and emittance are equal.

Convection heat transfer from the interior and exterior surfaces is calculated from correlations from the literature.[4] The coefficients are based on correlations that have been developed for isolated isothermal flat plates. The correlations are in the form of a Nusselt number (Nu) as a function of a Rayleigh number (Ra), a Grashof number (Gr), or a Reynolds number (Re), where

$$Nu = hL/k \tag{7}$$

$$Ra = g\beta\rho C_p \, \Delta T \, L^3/\nu k \tag{8}$$

$$Gr = Ra/Pr \tag{9}$$

$$Pr = \nu/\alpha \tag{10}$$

$$Re = V \, L/\nu \tag{11}$$

and

h = convection heat transfer coefficient

L = characteristic length of plate

k = thermal conductivity of air

g = acceleration of gravity

β = volume coefficient of expansion of air

ρ = density of air

C_p = specific heat of air

ΔT = temperature difference between surface and air

ν = kinematic viscosity of air

Pr = Prandtl number for air

α = thermal diffusivity of air

V = velocity of air stream

Since Nu, Ra, Gr, and Re are dimensionless numbers, any consistent set of units may be used to evaluate these quantities.

The model accounts for the temperature dependence of the properties of air by evaluating them at the film temperature, which is defined as the average of the temperatures of the surface and the air. Relationships for the temperature dependent properties of air were obtained from NBS Circular 564.[5]

The model utilizes correlations that have been developed for various orientations of the plate with respect to gravity, and for the

direction of heat flow (up vs down). Correlations for both laminar and turbulent flow are used, with the choice depending upon the magnitude of the Rayleigh number for natural convection and of the Reynolds number for forced convection. Separate coefficients are calculated for natural and forced flow, and a mixed coefficient is calculated by taking the third root of the sum of the cubes of the two separate coefficients.[6]

The correlations used in the model are given in Table 2.1. They account for the effects of the following variables: surface-to-air temperature difference, heat flow direction, film temperature, surface size, surface orientation and velocity of air flow past the plate. For exterior surfaces, the air speed is taken to be the wind speed obtained from meteorological data. For interior surfaces, the wind speed is taken to be zero. This crude estimate for interior air speed should suffice, since natural convection should dominate over forced convection there.

The latent heat term accounts for the heat associated with the condensation or evaporation of moisture at the outer surface of the roof. In its present form, the model does not account for moisture migration through the roof; it only accounts for condensation/evaporation at the outer surface. The latent heat term is obtained as the product of the rate of mass transfer at the surface, $\dot{m}_v$, and the latent heat of vaporization of water, h_v,

$$Q_{latent} = \dot{m}_v \, h_v \tag{12}$$

The mass transfer rate is given by

$$\dot{m}_v = h_m \, (W_{air} - W_s) \tag{13}$$

where

$\dot{m}_v$ = mass flow rate of moisture per unit area of roof

W = humidity ratio of the air or surface

h_m = mass transfer coefficient

Table 2.1. Correlations for convection coefficients (from Ref. 4).

I. Natural Convection:

A. Horizontal surface, heat flow up

$Nu = 0.54\ Ra^{1/4}$ for $Ra < 8 \times 10^6$

$Nu = 0.15\ Ra^{1/3}$ for $Ra > 8 \times 10^6$

B. Horizontal surface, heat flow down

$Nu = 0.58\ Ra^{0.2}$

C. Vertical surface

$Nu = 0.59\ Ra^{1/4}$ for $Ra < 1 \times 10^9$

$Nu = 0.10\ Ra^{1/3}$ for $Ra > 1 \times 10^9$

D. Nearly horizontal surface (tilt angle less than 2 degrees), heat flow down

$Nu = 0.58\ Ra^{0.2}$

E. Tilted surfaces (greater than 2 degrees tilt), heat flow down

$Nu = 0.56\ (Ra \cos(\varphi))^{1/4}$ φ = tilt angle

F. Tilted surface, heat flow up

$Nu = 0.56\ (Ra \cos(\varphi))^{1/4}$ for $Ra/Pr < Gr_c$

$Nu = 0.14\ (Ra^{1/3} - (Gr_c\ Pr)^{1/3})$
$+ 0.56\ (Ra \cos(\varphi))^{1/4}$ for $Ra/Pr > Gr_c$

$Gr_c = 1 \times 10^6$ for $\varphi < 15$ degrees

$Gr_c = 10**(\varphi/(1.1870 + 0.0870*\varphi))$
for 15 degrees $< \varphi <$ 75 degrees

$Gr_c = 5 \times 10^9$ for $\varphi > 75$ degrees

II. Forced Convection

$Nu = 0.664\ Pr^{1/3}\ Re^{1/2}$ for $Re < 5 \times 10^5$

$Nu = Pr^{1/3}\ (0.037\ Re^{0.8} - 850)$ for $Re > 5 \times 10^5$

The humidity ratios are calculated from psychrometric relations using known values of the relative humidity and temperature of the air and the temperature of the surface. When condensed moisture is present on the surface, it is assumed that the moisture in the air very near the surface is in equilibrium with the surface moisture. Therefore, the humidity ratio at the surface is taken to correspond to saturation conditions for the temperature of the surface. The mass transfer coefficient is obtained from the analogy between heat and mass transfer as

$$h_c/(h_m\ C_p) = (\alpha/D)^{2/3} \simeq 1 \tag{14}$$

where

h_c = convection heat transfer coefficient

C_p = specific heat of air

α = thermal diffusivity of air

D = coefficient for diffusion of water vapor through air

For this model, h_v has been taken to have a constant value of 1060 Btu/lb.

The system of equations represented by Equation 2 has a form such that temperatures at only three successive nodes are involved in each equation. Special equations are written for boundary nodes so that the boundary conditions are incorporated into the equations. When the explicit method of solution is used, the only unknown is the temperature at node P at the end of the time step. When either the fully implicit or the Crank-Nicolson method is used, each equation contains three unknowns (the temperatures at three successive nodes at the end of the step), thus requiring a solution of a set of simultaneous algebraic equations. The equations are written in a linear form with nonlinear terms such as those for radiation being factored into a quasilinear form. These simultaneous equations are solved in the STAR model using an efficient direct solution method known as the Thomas algorithm, or the tridiagonal matrix algorithm, which is described by Patankar.[3]

Iterative solutions are required because of temperature dependent thermal properties or because of nonlinear boundary conditions. When the thermal properties depend upon temperature, previous estimates of the nodal temperatures are used to estimate the thermal properties. Then new estimates for nodal temperatures are calculated, and these are used to obtain improved estimates of the thermal properties. This process is continued until succeeding estimates of the nodal temperatures agree to within a prespecified tolerance.

One nonlinear boundary condition is caused by the infrared radiation terms. This is linearized in the following manner. First, a temperature for the surroundings is defined as

$$T_{surr} = (Q_{infrared}/\sigma)^{1/4} \tag{15}$$

If values of the infrared radiation are not available, the model uses an algorithm based on the work of Martin and Berdahl to calculate an effective sky temperature which is taken to be the temperature of the surroundings.[7] The sky temperature is a function of the relative humidity, time of day, and cloud cover.

The absorbed infrared radiation and the emitted radiation are then combined to obtain the net infrared radiation gained by the surface as

$$\begin{aligned} Q_{IRnet} &= \epsilon\sigma(T_{surr}^4 - T_s^4) \\ &= \epsilon\sigma(T_{surr}^2 + T_s^2)\ (T_{surr} + T_s)\ (T_{surr} - T_s) \\ &= h_r\ (T_{surr} - T_s) \end{aligned} \tag{16}$$

In a manner similar to the treatment of temperature dependent thermal properties, the radiation coefficient h_r is estimated from previous estimates of the surface temperature. Then a new surface temperature is calculated and a new radiation coefficient is estimated until convergence is obtained. A similar treatment is used for the convection coefficients, which depend upon the surface temperature

through the temperature differential between the surface and the surrounding air.

The last nonlinearity involves the latent heat term through the dependence of the mass transfer at the surface on the temperature of the surface. This nonlinearity was handled by expanding the surface humidity ratio in a Taylor series such that

$$\begin{aligned} \dot{m}_v &= h_m (W_{air} - W_s) \\ &= h_m [W_{air} - W_s' - (dW_s/dT) (T_s - T_s')] \end{aligned} \tag{17}$$

where W_s' is the surface humidity ratio evaluated at a previously estimated surface temperature T_s'.

With either type of boundary condition, the model calculates temperatures at each of the nodes. If material properties vary with temperature, or if the weather boundary conditions are used, the model performs the calculations iteratively until it achieves a self-consistent set of nodal temperatures. With these nodal temperatures, the heat flows between nodes may be calculated.

2.2 COMPUTER IMPLEMENTATION

The STAR model has been implemented on an IBM AT personal computer. A general flow chart for the model is shown in Fig. 2.3, and a complete listing of the program is given in Appendix A. In the first step, basic input data are read. Two methods of reading this data have been provided. With the first method, the input data are entered interactively on the keyboard, with prompting questions being displayed on the monitor. With the other method, the same input data are read from an external file. Both methods are contained in a single computer program. A prompting question is displayed on the monitor to choose the method for a particular run of the model.

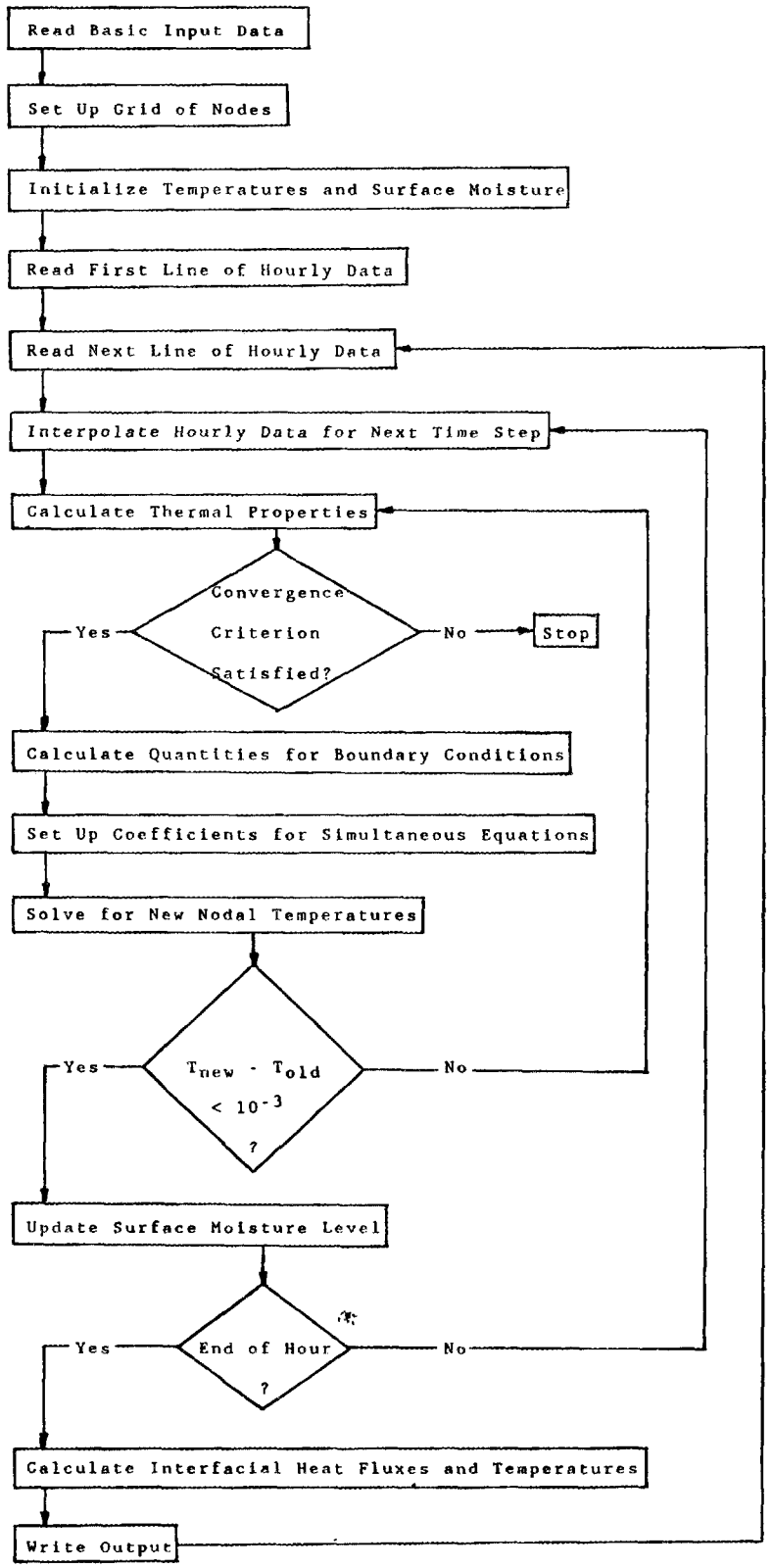

Fig. 2.3. Flow chart for STAR computer program.

The basic input data read in the first step are summarized in Table 2.2. An example of interactive input is given in Appendix B, and a corresponding external input file is given in Appendix C. The basic input data include geometrical information about the roof: its slope, length, and width. Next are the number of layers in the roof, and for each layer, the name of the material (not used at present), the thickness, number of nodes, thermal conductivity, specific heat, and density. The model is set up to accept the slope and intercept for thermal conductivities and specific heats that vary linearly with temperature. Constant properties may be used by entering a 0.0 for the slope.

The next item is the size of the time step for the transient solution. The program is set up to accept boundary data on an hourly basis and to calculate results on an hourly basis. However, the time step used in the solution can be smaller, with the provision that there be an integer number of time steps per hour. The next input is a flag to denote the type of solution method desired: either explicit, Crank-Nicolson, or fully implicit. The fully implicit method would usually be recommended, but the others are available if the user prefers them.

Next is a flag to specify the type of boundary condition on the outside surface. If the user chooses weather boundary conditions, then the following are needed: values for the solar absorptance and the infrared emittance, a choice of convection coefficients, and the choice of whether to include or ignore moisture condensation and evaporation at the outside surface. If the user does not want to use the correlations for convection coefficients that are built into the program, a constant value can be input. The next input is a flag to specify the type of boundary condition on the inside surface. If the user chooses room boundary conditions, the indoor temperature and a choice of convection coefficients are needed. Here again, the user may input a constant value for the inside convection coefficient.

Table 2.2. Data entered by keyboard or from external file.

1. Slope of roof, inches of rise per foot of run.
2. Length and width of roof, feet.
3. Number of layers in roof, limit of 20.
4. For each layer of the roof,
   a. Name of material
   b. Thickness, inches.
   c. Number of nodes, limit of 100.
   d. Thermal conductivity, slope and intercept for a linear variation with temperature, Btu-in./(hr-ft^2-^{o}F).
   e. Specific heat, slope and intercept for a linear variation with temperature, Btu/(lb-^{o}F).
   f. Density, lb/ft^3.
5. Size of time step, expressed as an integer number of time steps per hour of simulated time.
6. Choice of transient solution method: enter 0 for explicit, 0.5 for Crank-Nicolson, or 1.0 for fully implicit.
7. Choice of boundary conditions on outside surface: enter 0 for specified temperature or 1 for weather boundary conditions.
8. Solar absorptance and infrared emittance (only if weather boundary conditions are chosen), dimensionless.
9. Choice of a outside convection coefficient: enter 0 for user specified outside convection coefficient, or 1 for coefficients obtained from the built-in correlations (only if weather boundary conditions are chosen).
10. User specified outside convection coefficient (if needed), Btu/(hr-ft^2-^{o}F).
11. Choice to include or ignore the effects of latent heats at the outside surface: enter 0 to ignore or 1 to include.
12. Choice of boundary condition on inside surface: enter 0 for specified temperature or 1 for room conditions.
13. Indoor temperature (if room conditions chosen), ^{o}F.
14. Choice of inside convection coefficient: enter 0 for user specified inside convection coefficient, or 1 for coefficient obtained from correlations (only if room conditions are chosen).
15. User specified inside convection coefficient (if needed), Btu/(hr-ft^2-^{o}F).

After reading these inputs, the program sets up a grid of nodes and prints out on the monitor a listing of node numbers, distance of nodes from top of roof, and thickness of material associated with each node.

The nodal temperatures are then initialized to 75°F and the surface moisture level is initialized to 0.

Then the program reads the first line of hourly data. These are read from an external file of weather data which contains hourly values of the time, outdoor temperature, relative humidity, barometric pressure (not presently used), solar radiation, wind speed, and incident infrared radiation. In the case that values for the incident infrared radiation are not available, then this column should contain a value for the cloud amount, with a negative sign in front of it. The negative sign is a flag to instruct the program to use the algorithm for calculating an effective sky temperature. The programs are also set up to read an input file containing hourly values of the measured temperatures and heat fluxes. If necessary, the read statements for these two input files can be changed to meet specific needs of the user.

The next line of hourly data is then read. When the time step is less than an hour, linear interpolation is used to obtain boundary condition data between the hourly values.

In the next step, the thermal properties are calculated at each of the nodes using the most appropriate values for the nodal temperatures. With the explicit method, the properties are evaluated at the nodal temperatures from the previous time step. With the fully implicit method, the properties are evaluated using the most current estimate of the nodal temperatures. With the Crank-Nicolson methods, the properties are evaluated using an average of the temperatures from the previous time step and the most current values.

Following this, the convergence criterion is calculated for each node using Equation 3. This step is only performed once during a run, and it is completely bypassed with the fully implicit method. If any node fails the test, the program stops, and an error message is printed on the monitor. If any node is within a factor of two of failing the test, a warning message is printed on the monitor, but execution of the program continues.

A number of quantities associated with the boundary conditions are calculated next. The humidity ratios of the outside air and the roof outer surface are calculated using subroutine PSY1. An effective temperature for the surroundings is calculated with either Equation 15 or the algorithm for sky temperature, and then a radiative heat transfer coefficient is calculated using Equation 16. Convection heat transfer coefficients are calculated using subroutine HCON, and a mass transfer coefficient is calculated using subroutine HMASS. The latent heat terms are then calculated.

The coefficients for the simultaneous equations are computed, and then the equations are solved for new nodal temperatures. With either the fully implicit or the Crank-Nicolson method, the equations are solved using the tridiagonal matrix algorithm. The newly calculated nodal temperatures are compared with the previous estimates. If any of the new temperatures differs from the old temperature by more than 10^{-3} ^{o}F, the thermal properties are recalculated with the new temperatures and the process is repeated. However, the number of iterations is limited to 10.

When the temperatures have converged, the moisture level on the surface is updated, and the program moves on to the next time step. At the end of each hour of simulation, interfacial temperatures and heat fluxes are calculated and results are written to an output file. The output file contains hourly values of predicted temperatures and heat flows at all interfaces between materials and at the inside and outside surfaces of the roof.

2.3 INSTRUCTIONS FOR RUNNING PROGRAM

The first step is to prepare the necessary input file, either a file containing weather data or a file containing measured temperatures and heat fluxes. The weather file should contain hourly data in the following order: time, outdoor air temperature (^{o}F), relative humidity (percent), barometric pressure (inches mercury), total solar radiation on horizontal surface (Btu/(hr-ft^2)), wind speed (miles per hour), and total incident infrared radiation (Btu/(hr-ft^2)). If the incident infrared radiation is not available, the last column of this file should contain the cloud amount preceded by a minus sign. The cloud amount is a number between 0 (clear sky) and 10 (completely cloudy). A free format is used, but the data for each hour should be on separate lines. Also, the data should start on the second line.

The file of experimental data should contain hourly experimental data in the following order: time, measured temperatures at the surfaces and layer interfaces starting at the outside surface, and measured heat flux. A free format is also used for this file, and the data should start on the second line.

If the basic data are not input interactively from the monitor, an external file containing the basic input must also be prepared. This should follow the outline of Table 2.2. A free format may be used, but all data are entered on separate lines, except for the roof length and width which are entered on one line and the roof solar absorptance and infrared emittance which are entered on one line.

Prior to executing the program, the following commands should be issued:

SET OUT = filename to which output will be written

and

SET WEA = filename for weather file

and/or

SET EXP = filename for experimental data file
depending upon which mode of operation is being used.

To execute the program in the interactive mode, enter

STAR

A series of prompts will then be displayed on the monitor, and the corresponding input data should be entered.

To execute the program using an external input file, issue the commands

SET IN = filename for external file
STAR

The program will then execute. At certain points, information will be displayed on the screen to monitor the progress of the program. After some of these, an instruction will be displayed to press the ENTER or RETURN key to continue. Execution can be terminated at any point by pressing CTRL-BREAK.

2.4 PLANS FOR FURTHER DEVELOPMENT

While the STAR model is useful at present, it will continue to be developed. In its present form, the user must supply values for the material properties. It is planned to build a library of material properties into the program from which the user may select values. It is also planned to add other phenomena to the model. These will include the migration of moisture through the roof, rather than just condensation and evaporation at the outer surface. Migration of moisture will be modeled as diffusion and convection of moisture between nodes, with storage and release of moisture at the nodes. Storage and release of moisture will be accompanied by latent heat effects which will be coupled with the thermal model. The moisture

migration model will allow predictions of condensation, evaporation, freezing, and thawing through the thickness of the roof system. The model will also be coupled with other models for determining induced mechanical strains and stresses in the roof system. For this coupling, temperature patterns calculated with the thermal model will be used as inputs to mechanical models.

3. COMPARISON OF MODEL WITH EXPERIMENT

The STAR model has been verified by comparing its predictions with experimental data collected at the Roof Thermal Research Apparatus (RTRA). This section gives a description of the experimental setup, experimental results, and a comparison of the model predictions with the data.

3.1 EXPERIMENTAL SETUP

The RTRA is housed in a concrete block building approximately 8 feet wide by 26 feet long by 9 feet high. The RTRA has an insulated concrete slab-on-grade floor. The roof consists of a central fixed built-up roof (BUR) with four 4 foot by 8 foot test sites, two on each side. The interior temperature of the RTRA is controlled at about 75°F.

A cross section of the panel used for comparisons with the model is shown in Fig. 3.1. It consisted of four 15/16 inch sheets of fiberglass insulation over an 18 gauge metal roof deck. The top surface was sealed with a modified bitumen membrane. This cross section also shows a layer of concrete pavers above the insulation and membrane. The panel was divided into two 4 foot by 4 foot sections. One section was left bare and the other section had the concrete pavers. The bitumen cover was added to the pavers in order to match the radiative properties of the two panel sections. Near the center of each section, thermocouples were located at the exterior boundaries and between each layer of the panel. Calibrated heat flux transducers were located between the two inner layers of insulation near the center of each section.

In addition to the temperatures and heat fluxes measured on the panel, weather data were collected at the site. These consisted of outdoor temperature, relative humidity, wind speed, barometric

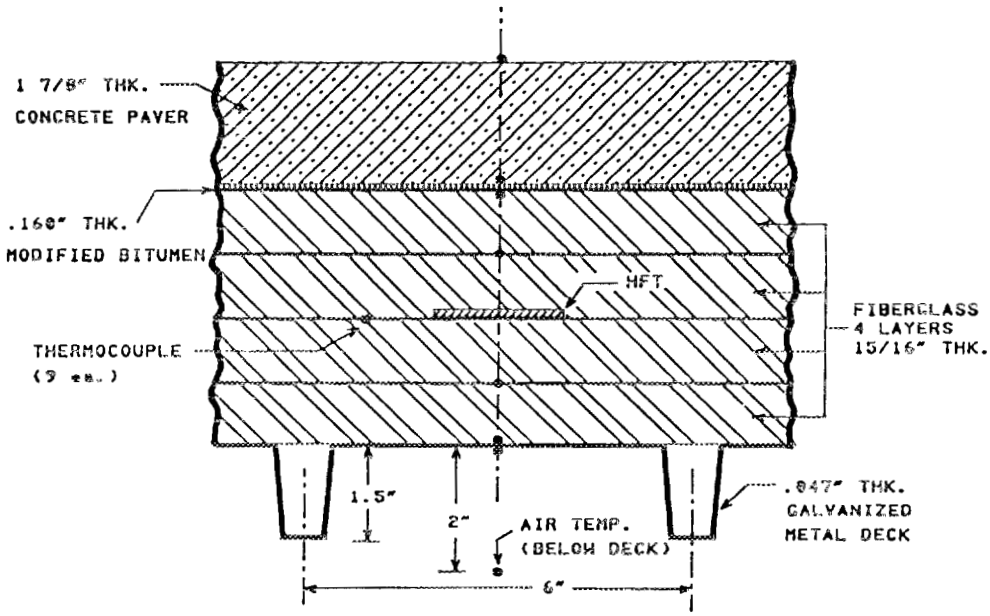

Fig. 3.1. Cross section of experimental roof panels.

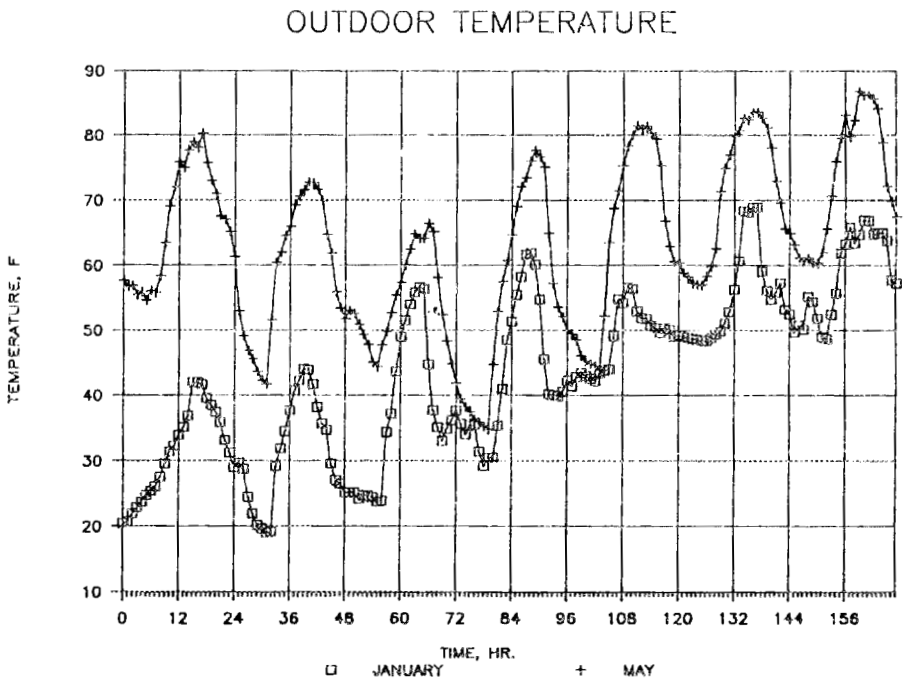

Fig. 3.2. Measured outdoor temperatures.

pressure, incident solar radiation (pyranometer measurements over the 0.28 to 2.8 micron wavelength range), and incident infrared radiation (pyrgeometer measurements over the 4 to 50 micron wavelength range). These data were monitored continuously and hourly averages were recorded.

3.2 EXPERIMENTAL RESULTS

Two weeks of data were selected for comparison with the model predictions. They correspond to a cool week (January 29 - February 4, 1986) and a warm week (May 1 - May 7, 1986). Measured ambient air temperatures for these two periods are shown in Fig. 3.2. During the week in January, the ambient temperature varied between 19 and 69°F, and exhibited a warming trend. During May, relatively warm days and cool nights prevailed with ambient temperatures varying between 35 and 88°F. Measured incident solar radiation values are shown in Fig. 3.3. The January time period exhibited both cloudy and sunny conditions while the week in May had predominantly clear skies. Measured incident infrared radiation data are shown in Fig. 3.4. The large magnitude of the infrared radiation should be noted. On cloudy days it can exceed the peak solar radiation. The pyrgeometer measures only the incident infrared radiation, not the net amount which includes the outgoing radiation emitted and reflected by the surface.

The two quantities examined in this report are the temperature between the membrane and the insulation, and the heat flux through the roof. This temperature is important because it influences the useful lives of the membrane and the insulation and the choice of materials for these two components. The heat flux through the roof determines the magnitude of any energy savings. Measured values for the membrane temperature for the week in May are shown in Fig. 3.5. This figure shows temperatures for both the bare roof and the roof loaded with the concrete pavers. The paver results in a decreased amplitude for the temperature fluctuations experienced by the membrane. The peak daytime temperatures with the paver are as much as 30°F lower than with the

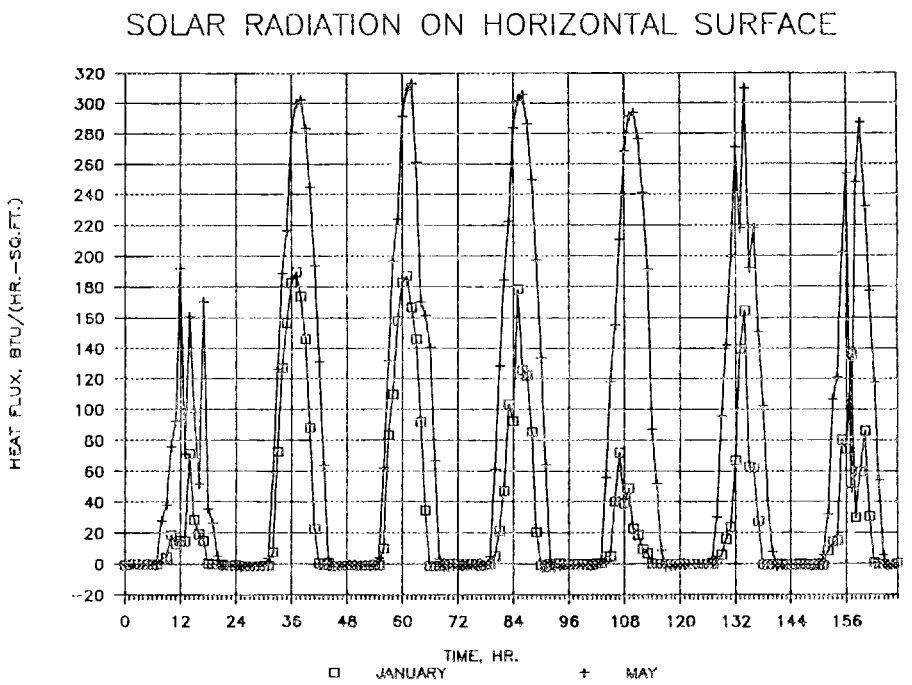

Fig. 3.3. Measured solar radiation.

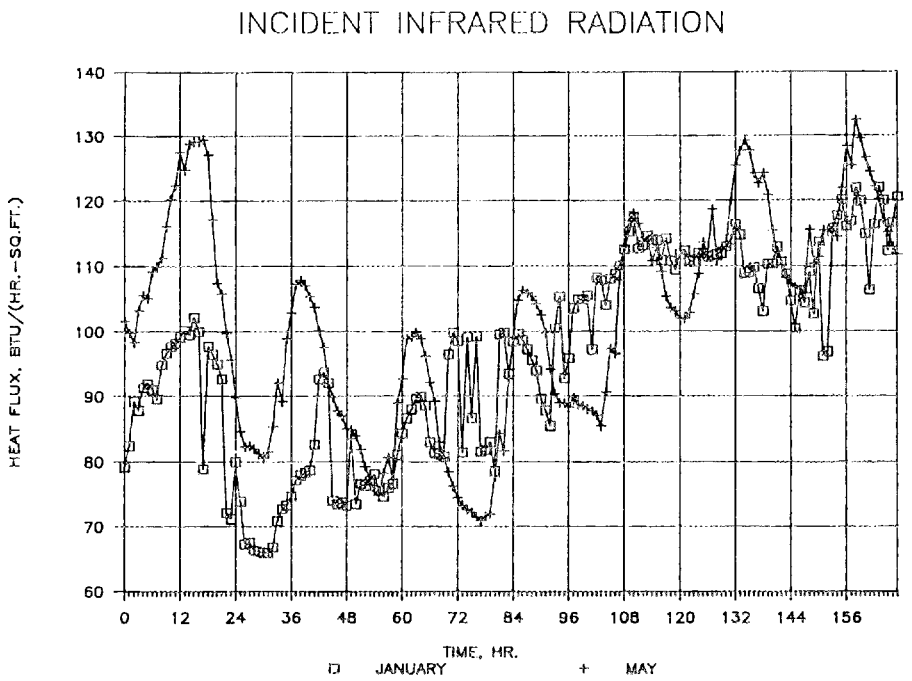

Fig. 3.4. Measured incident infrared radiation.

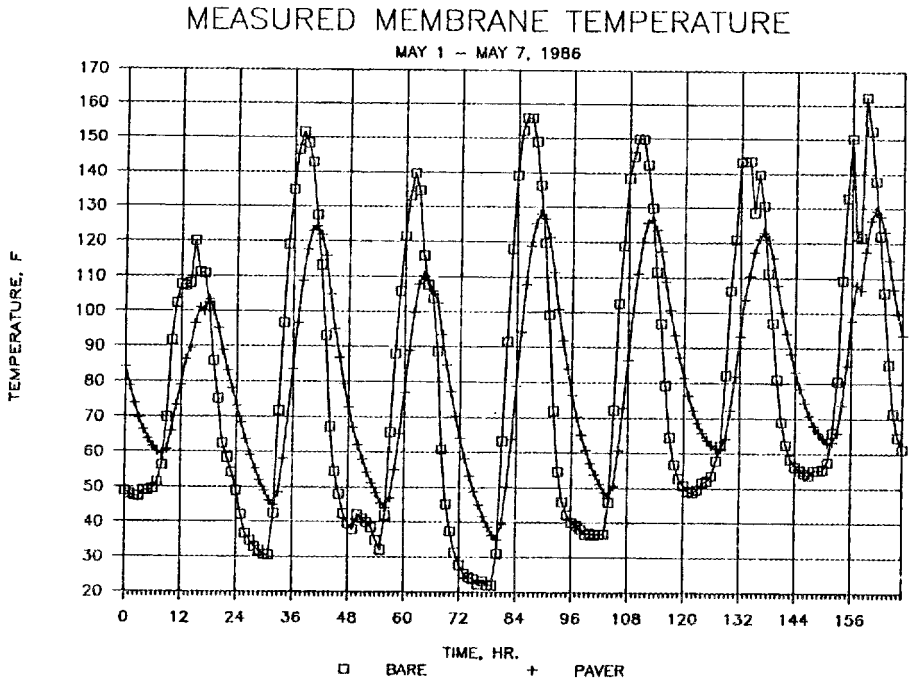

Fig. 3.5. Measured membrane temperatures.

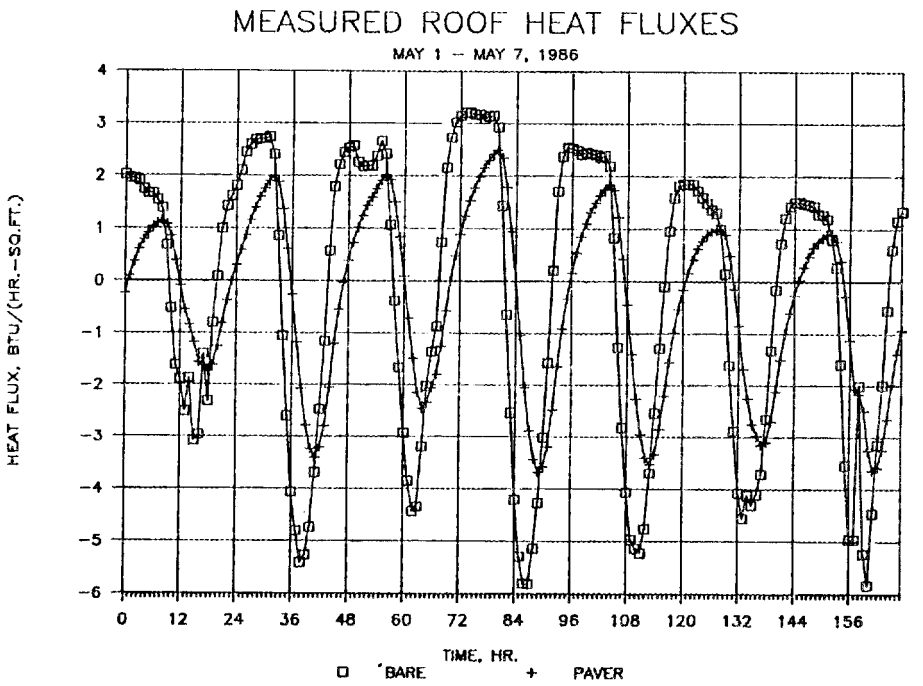

Fig. 3.6. Measured roof heat fluxes.

bare roof. The pavers also reduce the nighttime temperature extremes. In some cases, such reductions in temperature extremes might be critical to extending the life of the membrane, or in allowing an alternate selection of membrane and/or insulation materials.

Roof heat fluxes measured for the week in May are compared in Fig. 3.6. Here, heat flow out of the building is positive while heat fluxes into the building are assigned negative values. The added mass reduces the peak heat flows in both the positive and negative directions. The presence of the pavers can also be seen to delay the occurrence of the peak heat flows by one to two hours. Whether the effect of mass on energy consumptions during this period is beneficial or not will depend upon the thermal behavior and operation of the rest of the building.

3.3 MODEL VERIFICATION

The validity of the model has been assessed by comparing its predictions with the measured membrane temperatures and roof heat fluxes. Values used for the geometry and material properties are given in Table 3.1. The solar absorptance value was determined from in-house measurements. The other property values are taken from References 8 and 9. All calculations were performed using the fully implicit technique, using a time step of 0.1 hours. A few runs were made with time steps of 1 hour and 0.01 hours, with more and fewer nodes to verify that the node spacings and time step used were satisfactory. To eliminate the effects of the initial conditions, an artificial period of three extra days was added at the beginning, by repeating the boundary conditions that applied to the first day of the simulation period. Output heat flux and temperature predictions for the three additional 24-hour periods were discarded.

In the first step of this assessment, the model was run using measured temperatures for boundary conditions at the inside surface and at various planes within the bare and paver roof panels. Measured and

Table 3.1. Material properties and geometric values used in models.

Material	Thickness in.	Number of Nodes	Thermal Conductivity, BTU-in/(hr-ft^2-^{o}F)	Specific Heat, BTU/(lb-^{o}F)	Density, lb/ft^3
Modified Bitumen*	0.160	1	1.14	0.35	67.5
Concrete	1.875	4	12.0	0.22	140.0
Modified Bitumen*	0.2225	1	1.14	0.35	67.5
Fiberglass Insulation	3.75	8	0.254	0.23	13.2

* Solar Absorptance = 0.84
Infrared Emittance = 0.9

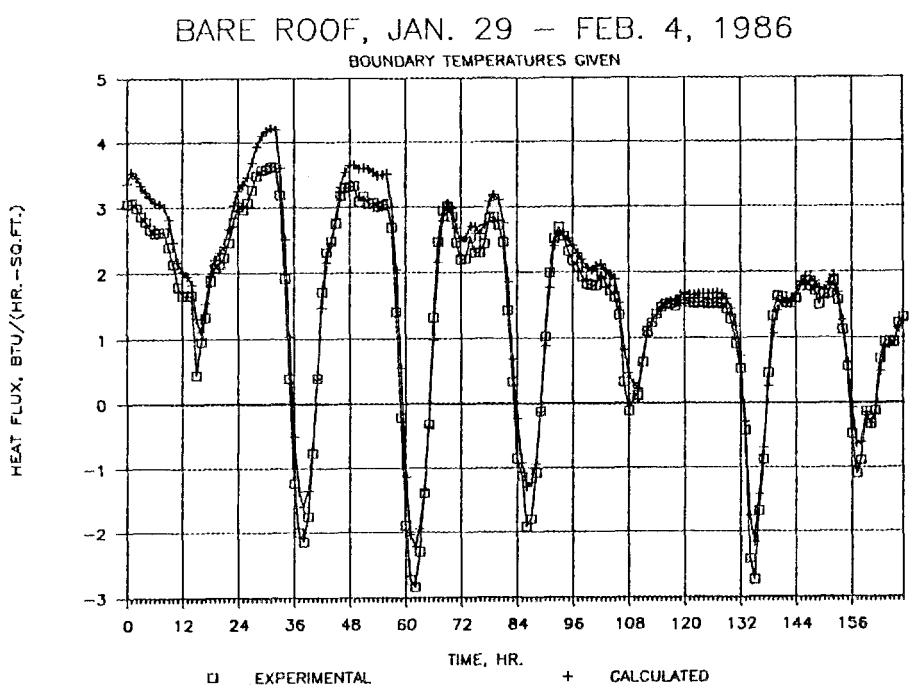

Fig. 3.7. Comparison of predicted and measured roof heat fluxes for bare roof in cool weather with given boundary temperatures at top of membrane, using constant thermal properties.

predicted heat flows for the bare roof during the week in winter are shown in Figs. 3.7 through 3.9. For Fig. 3.7, the temperature at the outer surface of the roof panel was used as a boundary condition, and the thermal properties were taken to be independent of temperature, as given in Table 3.1. Figure 3.8 shows the heat flows calculated using the measured temperature at the membrane/insulation interface as a boundary condition. It was noticed that the temperatures measured at this interface were sometimes higher than those measured on top of the membrane during the peak daytime hours. Because of the difficulties of accurately measuring surface temperatures, the interface temperatures are probably more accurate. Using the interface temperatures as a boundary condition tends to improve the predictions at the peak daytime hours. Still, it is apparent from Fig. 3.8 that the predicted heat flows during the peak daytime hours are too low and those at the nighttime hours are too large. As the next step, a temperature dependent thermal conductivity for the fiberglass insulation was used, given by

$$k = 0.20525 + 0.00065\ T \tag{18}$$

This equation is forced to give the same value of k at 75°F as is listed in Table 3.1. The slope of the conductivity versus temperature is estimated from Reference 8. Results using the temperature dependent thermal conductivity and the measured temperature at the membrane/insulation interface are given in Fig. 3.9. By comparing Figs. 3.8 and 3.9, it is apparent that the use of a temperature dependent thermal conductivity produces significant improvements in the prediction of the heat flux, especially during the nighttime hours when the insulation temperatures are very cold.

The same sequence of model runs was performed for the bare roof for the week in spring. Results using temperature independent properties and the temperature at the top of the membrane as a boundary condition are given in Fig. 3.10. For this week, the use of the

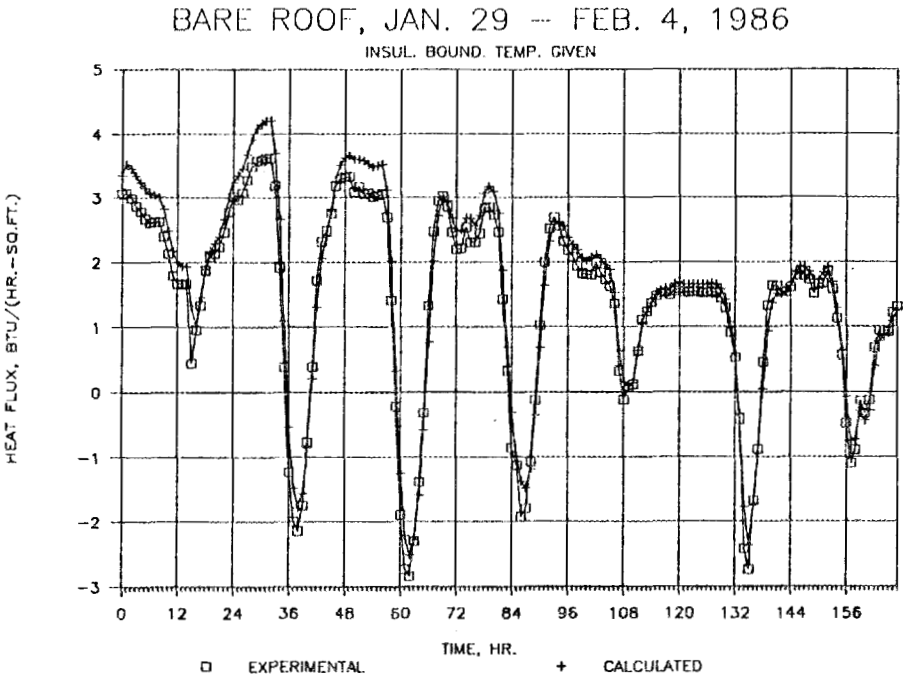

Fig. 3.8. Comparison of predicted and measured roof heat fluxes for bare roof in cool weather with given boundary temperatures at top of insulation, using constant thermal properties.

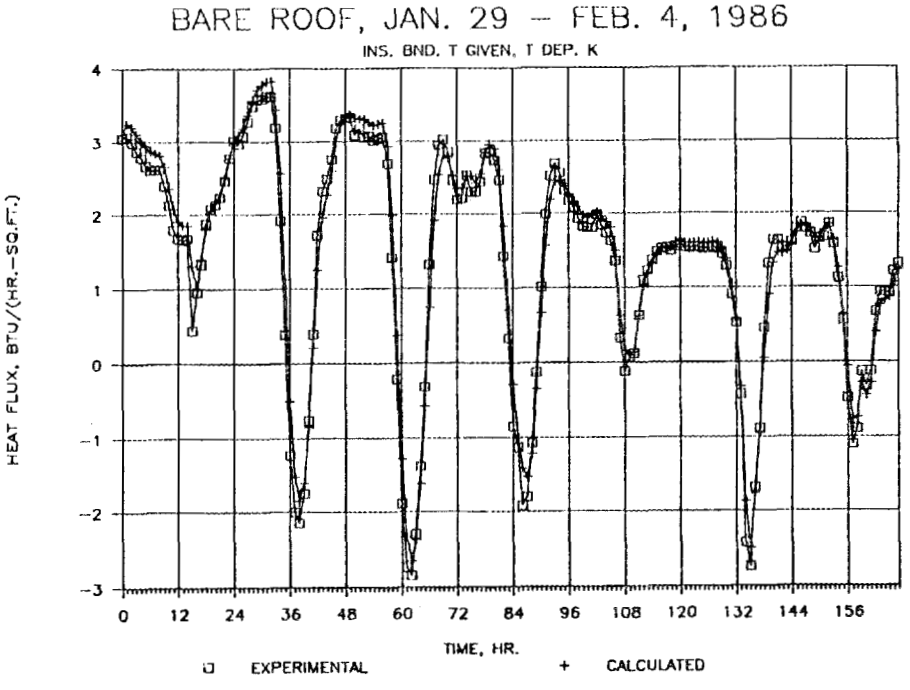

Fig. 3.9. Comparison of predicted and measured roof heat fluxes for bare roof in cool weather with given boundary temperatures at top of insulation, using temperature-dependent insulation thermal conductivity.

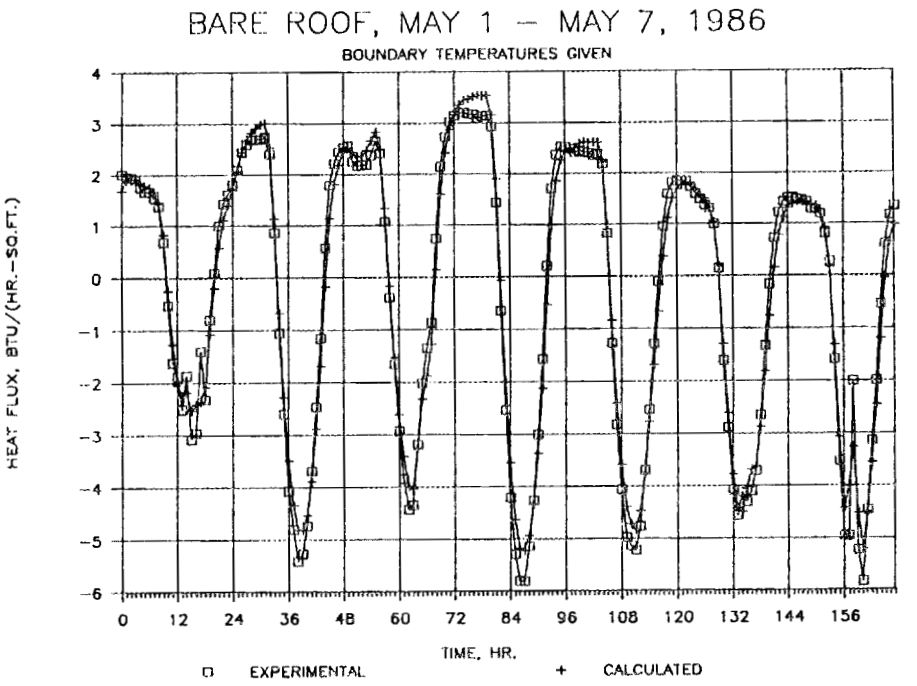

Fig. 3.10. Comparison of predicted and measured roof heat fluxes for bare roof in warm weather with given boundary temperatures at top of membrane, using constant thermal properties.

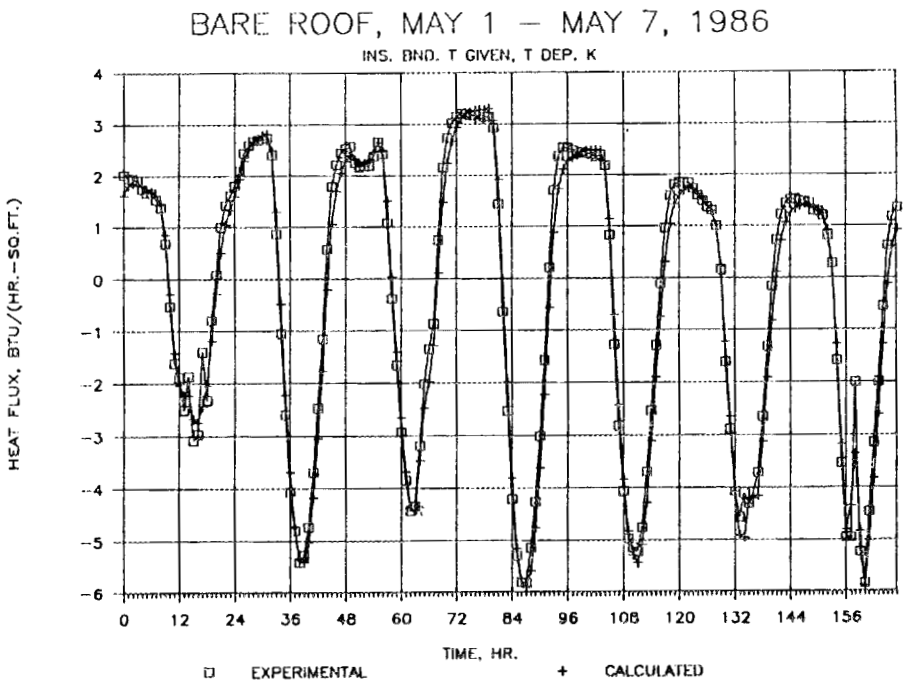

Fig. 3.11. Comparison of predicted and measured roof heat fluxes for bare roof in warm weather with given boundary temperatures at top of insulation, using temperature-dependent insulation thermal conductivity.

membrane/insulation interface temperature was found to produce only a small improvement over using the temperature at the outer surface as a boundary condition. However, the use of a temperature dependent thermal conductivity produces noticeable improvements, especially during the nighttime hours, as shown in Fig. 3.11. Considering the results given in Figs. 3.9 and 3.11 as the most realistic, it is seen that the model predictions are in very good agreement with the experimental data. This indicates that the model is properly simulating the heat transfer processes through the fiberglass insulation.

Two sets of simulations were performed for the roof panel with the heavy paver. Both sets used the temperature dependent thermal conductivity of the fiberglass insulation, and temperature independent values for the other material properties. One set of simulations was performed using the temperature measured at the top of the insulation as a boundary condition. The other set of simulations was performed using the temperature measured at the top of the paver as the boundary condition, with the results shown in Figs. 3.12 and 3.13. Since results from the first set of simulations were very similar, plots are not presented here. Both of these sets of simulations show very good agreement between the predicted and measured values of heat flow, confirming that the heat transfer processes across the stack of insulation, membrane, and paver are being modeled properly.

As the next step, the weather boundary conditions on the exterior side were used instead of the measured boundary temperatures. For all these simulations, the temperature dependent thermal conductivity for the fiberglass insulation was used. Measured and predicted temperatures at the membrane/insulation interface are shown in Fig. 3.14 for the bare roof during the week in winter, and measured and predicted heat flows are shown in Fig. 3.15. From these two figures, the most obvious differences between the predicted and measured values are that the predicted temperatures are too low during the coldest

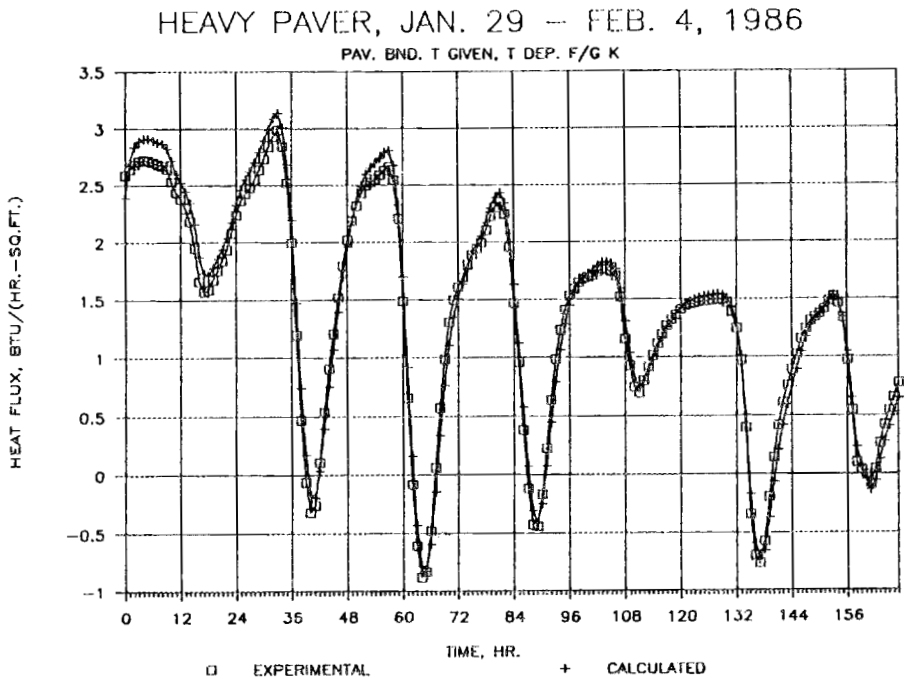

Fig. 3.12. Comparison of predicted and measured roof heat fluxes for paver roof in cool weather with given boundary temperatures at top of paver, using temperature-dependent insulation thermal conductivity.

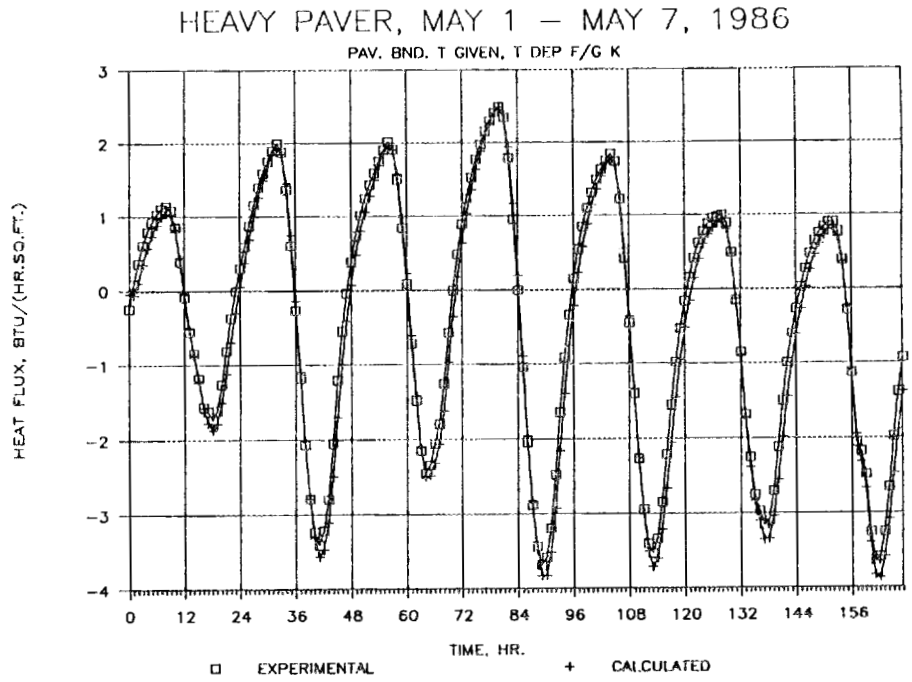

Fig. 3.13. Comparison of predicted and measured roof heat fluxes for paver roof in warm weather with given boundary temperatures at top of paver, using temperature-dependent insulation thermal conductivity.

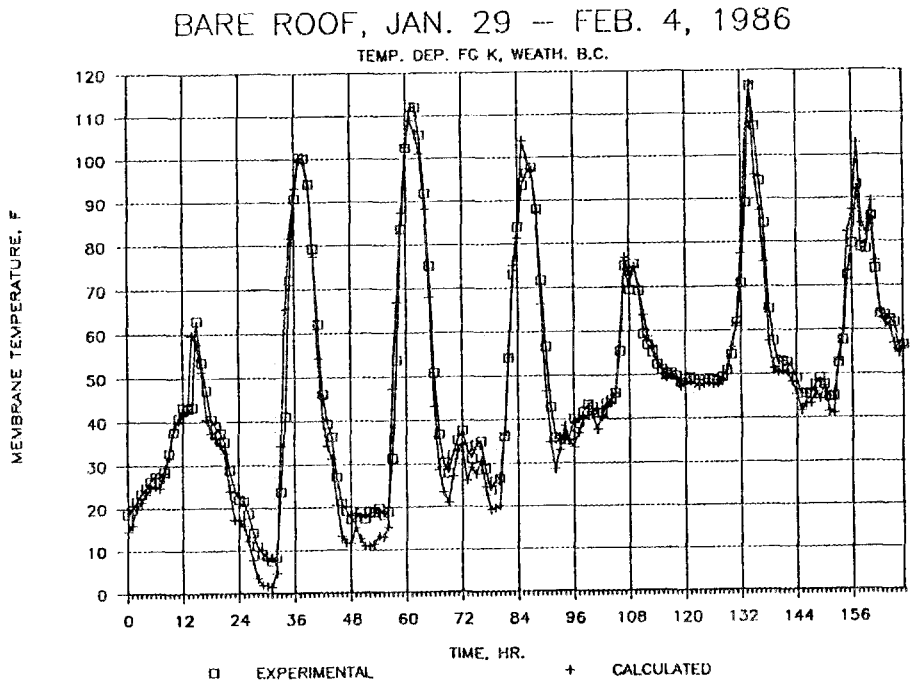

Fig. 3.14. Comparison of predicted and measured membrane temperatures for bare roof in cool weather with weather boundary conditions, using temperature-dependent insulation thermal conductivity.

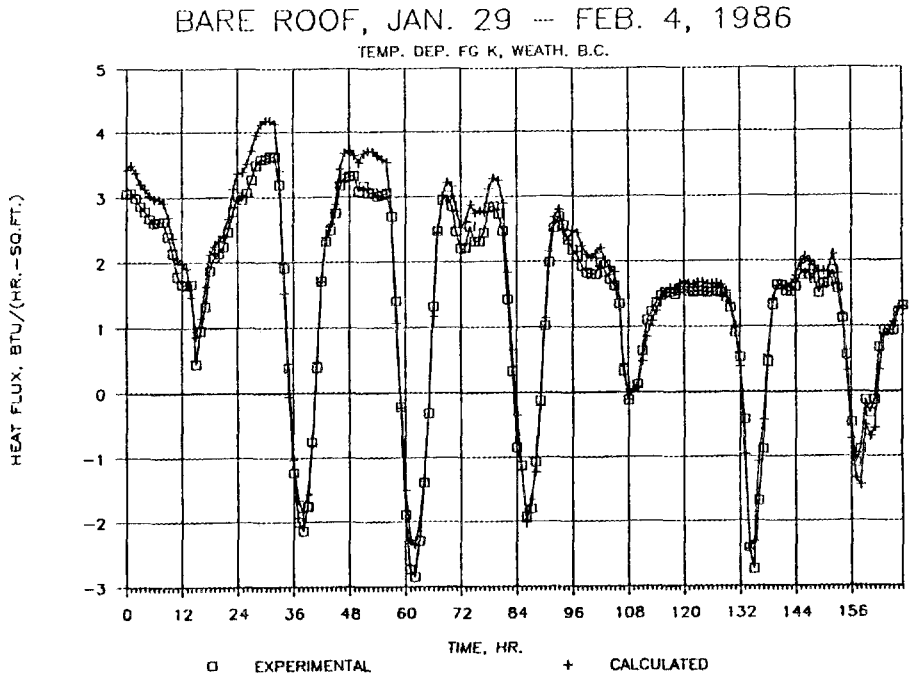

Fig. 3.15. Comparison of predicted and measured roof heat fluxes for bare roof in cool weather with weather boundary conditions, using temperature-dependent insulation thermal conductivity.

nighttime hours, and as a consequence, the predicted heat flows are too high during these same hours. Otherwise, there is very good agreement between the calculated and measured values.

Two factors were identified that might explain the differences between the measured and predicted values during the cold nighttime hours. The first is that the relative humidity sensor was not operating properly during the week in winter. The sensor reading was always close to 50 percent relative humidity, while it is likely that the relative humidity reached fairly high values during the nighttime hours. It can be argued that if the humidity was higher that thought, then more moisture could condense at the surface. The latent heat given up by the condensing moisture would help keep the surface warmer and thus reduce the heat flows at night. To test this hypothesis, the model was run using a constant relative humidity of 100 percent. The results showed only minor improvements in the agreement between predicted and measured heat flows.

The second factor is related to the relative humidity in a secondary way. The incident infrared radiation is measured with a pyrgeometer. This instrument has a silicon dome that is transparent to infrared radiation. During the nighttime hours when the relative humidity is high, moisture condenses on the dome. Since water is relatively opaque to infrared radiation, the instrument would not measure the true amount of incident radiation, and would probably read too low a value. When this low value of incident infrared radiation is used in the model, the model would predict surface temperatures that are too low also. When the sun rises, solar radiation evaporates the condensed moisture from the dome so that the infrared readings through most of the daytime hours would be accurate. To investigate this hypothesis, a simulation was performed where the measured nighttime infrared radiation was replaced with radiation from surroundings at the temperature of the ambient air. Results from this simulation are given in Fig. 3.16. Comparing Figs. 3.15 and 3.16, it is apparent that

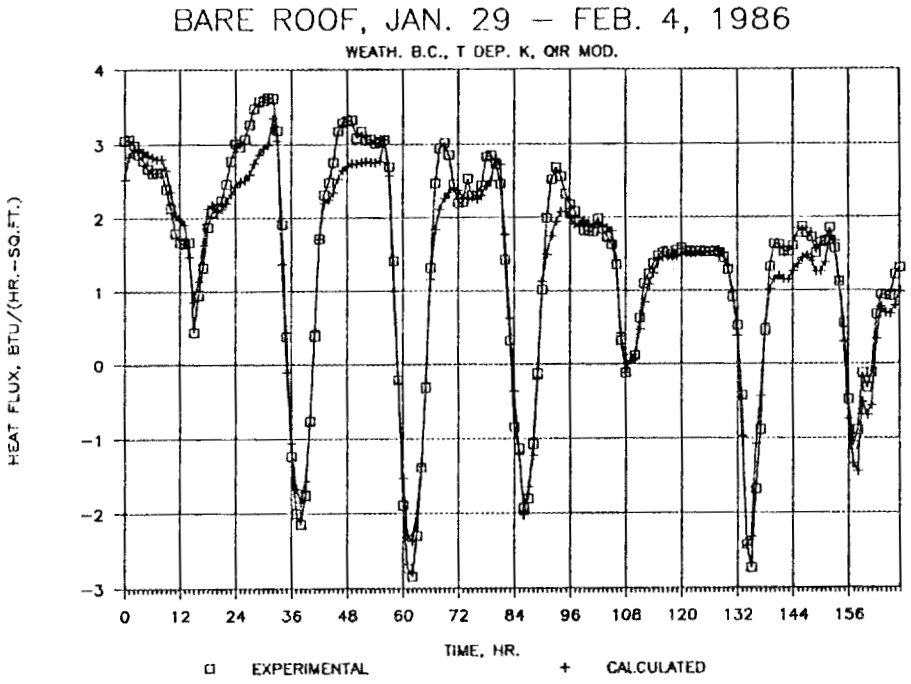

Fig. 3.16. Comparison of predicted and measured roof heat fluxes for bare roof in cool weather with weather boundary conditions, using temperature-dependent insulation thermal conductivity and modified infrared radiation.

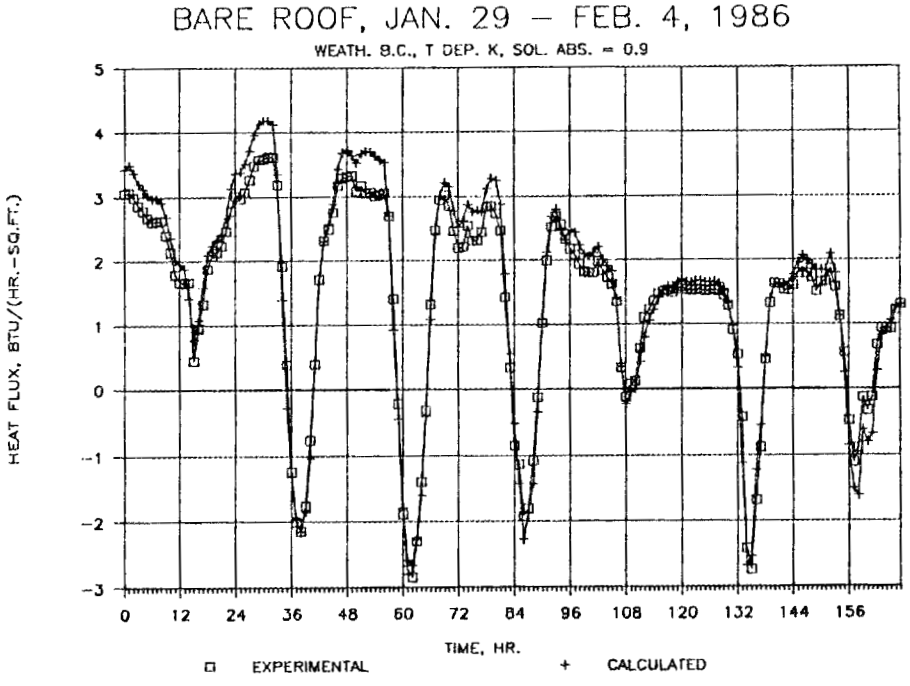

Fig. 3.17. Comparison of predicted and measured roof heat fluxes for bare roof in cool weather with weather boundary conditions, using temperature-dependent insulation thermal conductivity and solar absorptance of 0.9.

the nighttime incident infrared radiation has a significant effect on the heat flows through the roof during the nighttime hours. The measured heat flows are about midway between those predicted using the measured incident infrared radiation and those predicted using an incident infrared radiation from surroundings at the same temperature as the outdoor air. Since the two predictions bracket the measured values, it appears that the deviations between measured and predicted values during the nighttime hours are due to uncertainties in the incident infrared radiation.

Two other sensitivity analyses were performed for the bare roof for the week in the winter. In one set, the roof solar absorptance was set at 0.8 for one simulation, and at 0.9 for the other simulation. These two values bracket the nominal value of 0.84 that was used for the other simulations. It was found that the solar absorptance has a moderate effect on the heat flows during the peak daytime hours. The best fit to the data was obtained with a solar absorptance of 0.9, as shown in Fig. 3.17.

In the other sensitivity analysis, the value for the outside surface convection heat transfer coefficient was varied. In one run, the coefficients were increased by 20 percent over their usual value, and in the other run they were decreased by 20 percent. It was found that the heat flow is most sensitive to the convection heat transfer coefficient during the peak daytime hours, and that the best fit to the measured data is obtained by using a coefficient that is about 20 percent lower than the usual values that are calculated from the correlations given in the literature. Results for these calculations are given in Fig. 3.18. Since the calculated values in Figs. 3.17 and 3.18 are similar, it is not clear whether the discrepancy between peak daytime heat fluxes shown in Fig. 3.15 are due to the solar absorptance or to the convection coefficients that were used.

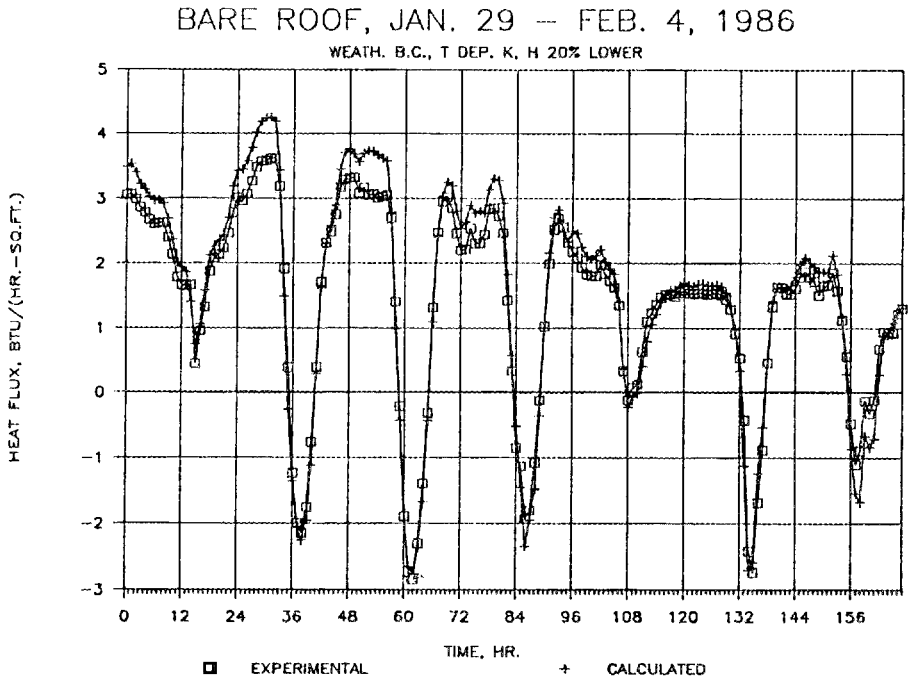

Fig. 3.18. Comparison of predicted and measured roof heat fluxes for bare roof in cool weather with weather boundary conditions, using temperature-dependent insulation thermal conductivity and convection coefficient 20 percent lower than normal.

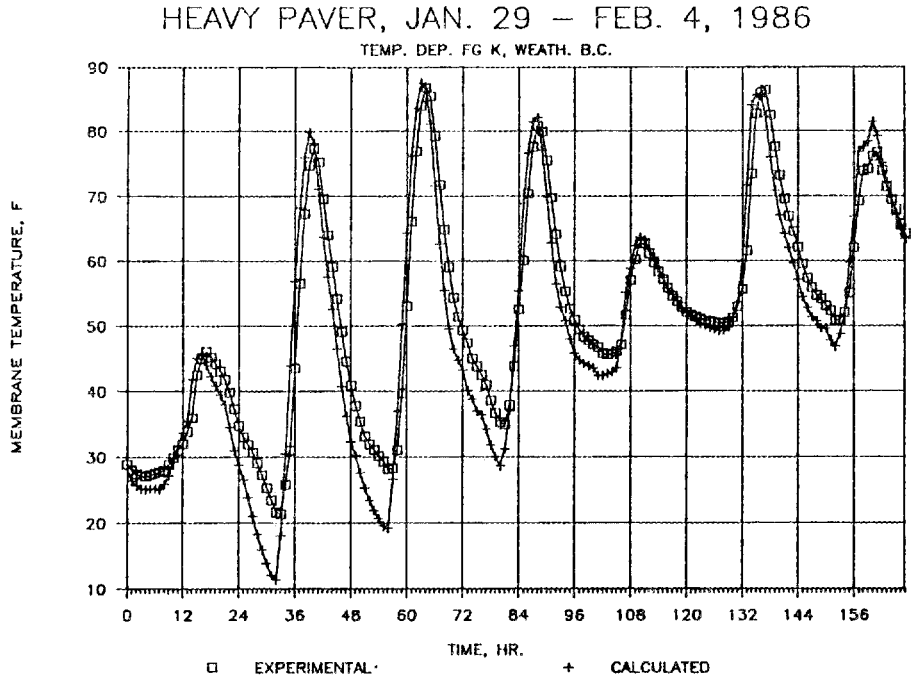

Fig. 3.19. Comparison of predicted and measured membrane temperatures for paver roof in cool weather with weather boundary conditions, using temperature-dependent insulation thermal conductivity.

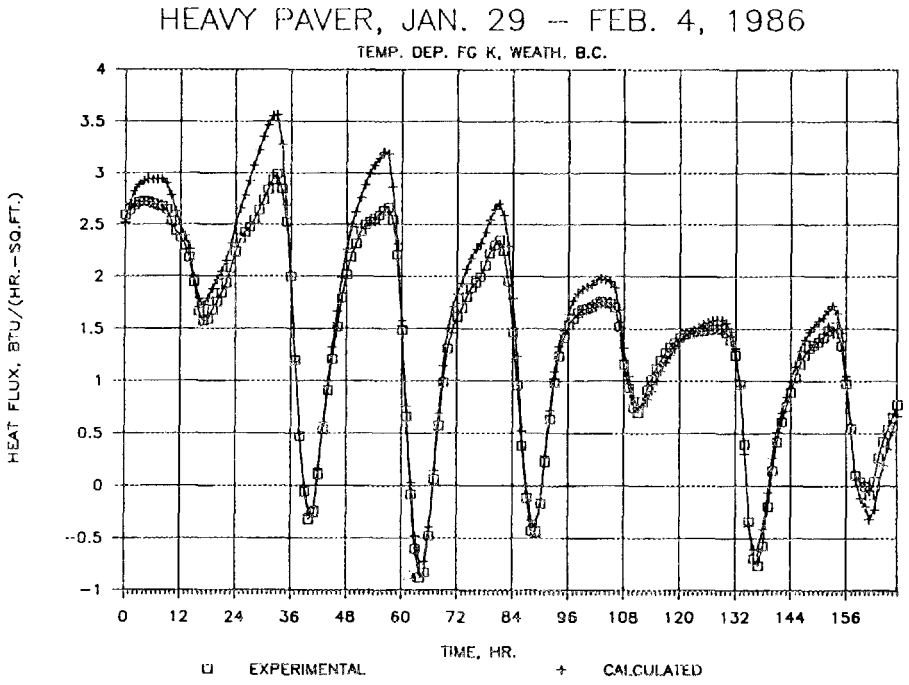

Fig. 3.20. Comparison of predicted and measured roof heat fluxes for paver roof in cool weather with weather boundary conditions, using temperature-dependent insulation thermal conductivity.

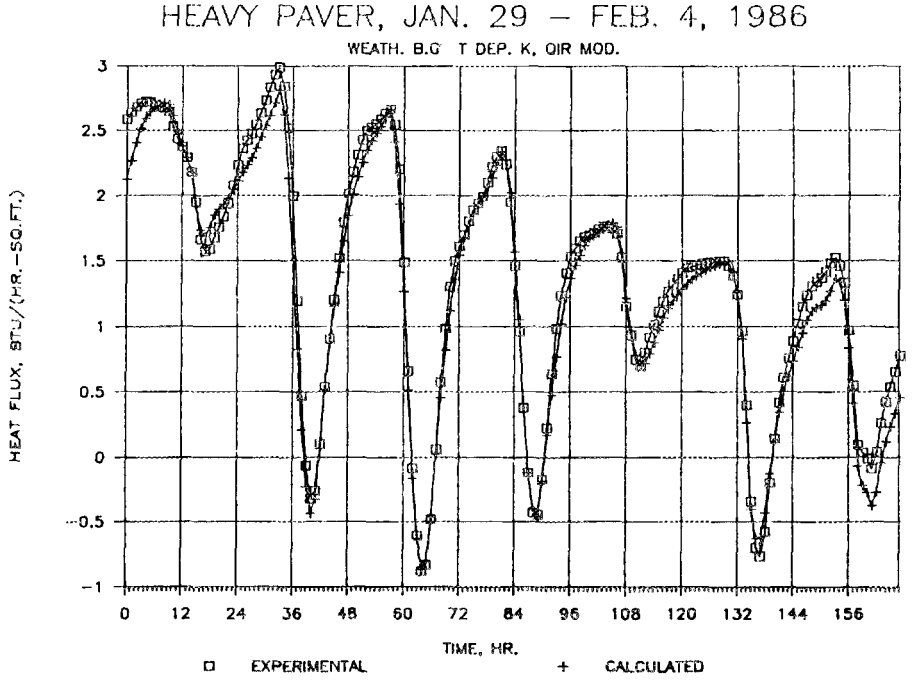

Fig. 3.21. Comparison of predicted and measured roof heat fluxes for paver roof in cool weather with weather boundary conditions, using temperature-dependent insulation thermal conductivity and modified infrared radiation.

Figures 3.19 and 3.20 show a comparison of predicted and measured values for the membrane/insulation interface temperature and the roof heat flux for the heavy paver panel for the week in winter. The temperature dependent fiberglass thermal conductivity was used for both these figures. These figures show that the predicted nighttime membrane temperatures are too low and as a consequence, the predicted heat fluxes are too high. Otherwise, there is good agreement between predicted and measured values. Another simulation was performed using a nighttime incident infrared radiation that corresponds to radiation from surroundings at the outdoor air temperature, as was done for the bare roof. The heat fluxes predicted with this run are shown in Fig. 3.21. The measured nighttime heat fluxes are bracketed by these two predictions, with the predictions made with the modified infrared radiation being closer to the measured values.

The sequence of simulations made for the heavy paver roof in the winter was repeated for both the bare roof and the heavy paver roof in the spring. These results are shown in Figs. 3.22 through 3.27. For Figs. 3.24 and 3.27, the nighttime infrared radiation has been changed as was done above, and also the solar absorptance has been reduced from 0.84 to 0.7. These results show that the two methods of treating the infrared radiation bracket the heat fluxes measured during the nighttime hours. Also, the use of a lower solar absorptance produces better agreement during the peak daytime hours. Although these observations are not conclusive, they suggest that the solar absorptance of the outer membrane may have changed between the winter tests and the spring tests as the membrane aged.

Table 3.2 presents a comparison of the predicted peak membrane temperatures and the weekly total heat flows for both types of roof. These comparisons were made using the temperature dependent thermal conductivity of fiberglass insulation, and the weather data as measured. Except for a few cases, the predicted values are in good agreement with the measured values. The most notable exceptions are

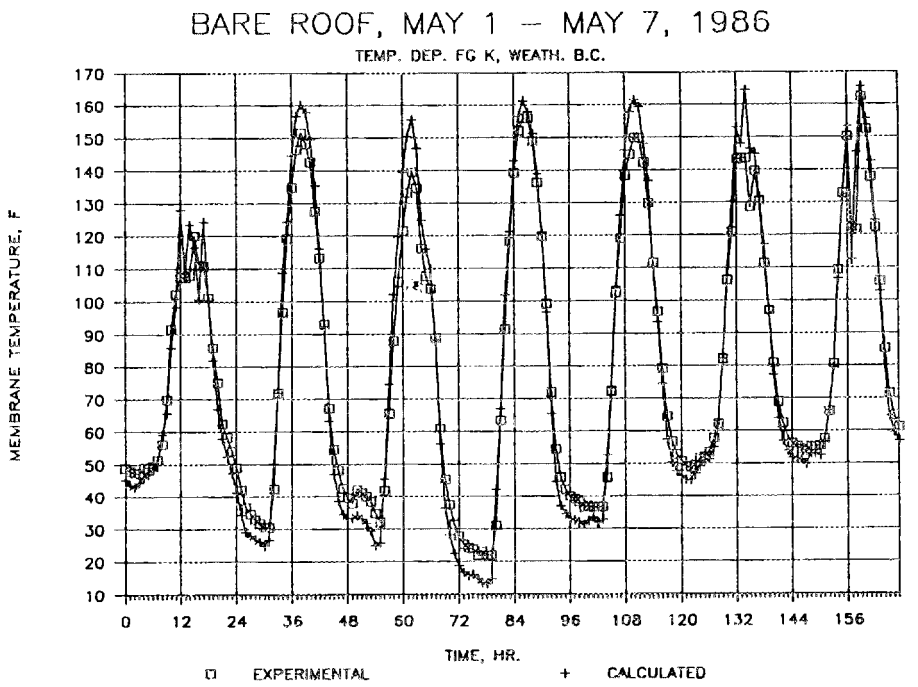

Fig. 3.22. Comparison of predicted and measured membrane temperatures for bare roof in warm weather with weather boundary conditions, using temperature-dependent insulation thermal conductivity.

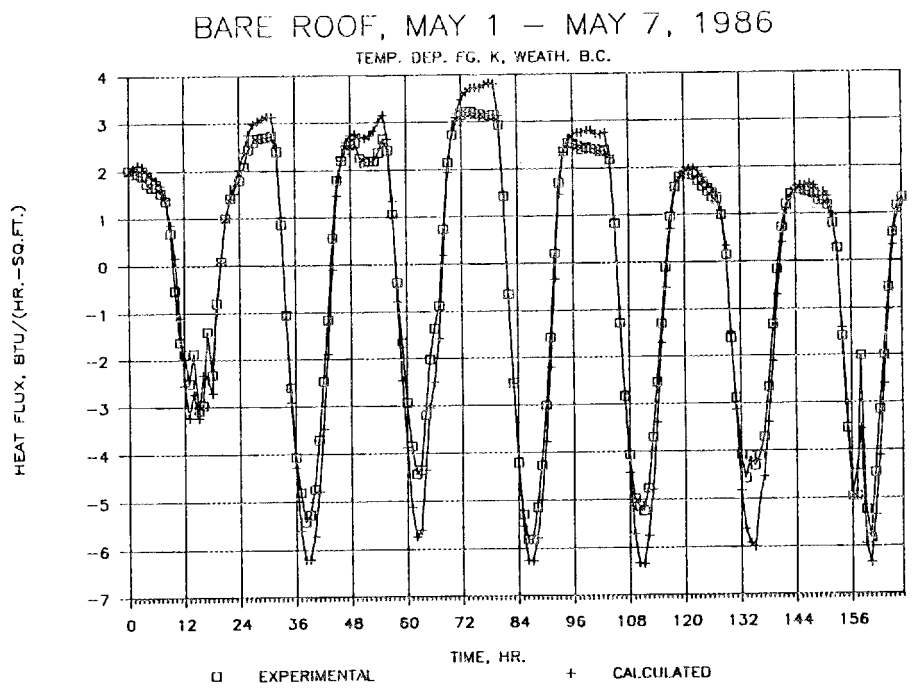

Fig. 3.23. Comparison of predicted and measured roof heat fluxes for bare roof in warm weather with weather boundary conditions, using temperature-dependent insulation thermal conductivity.

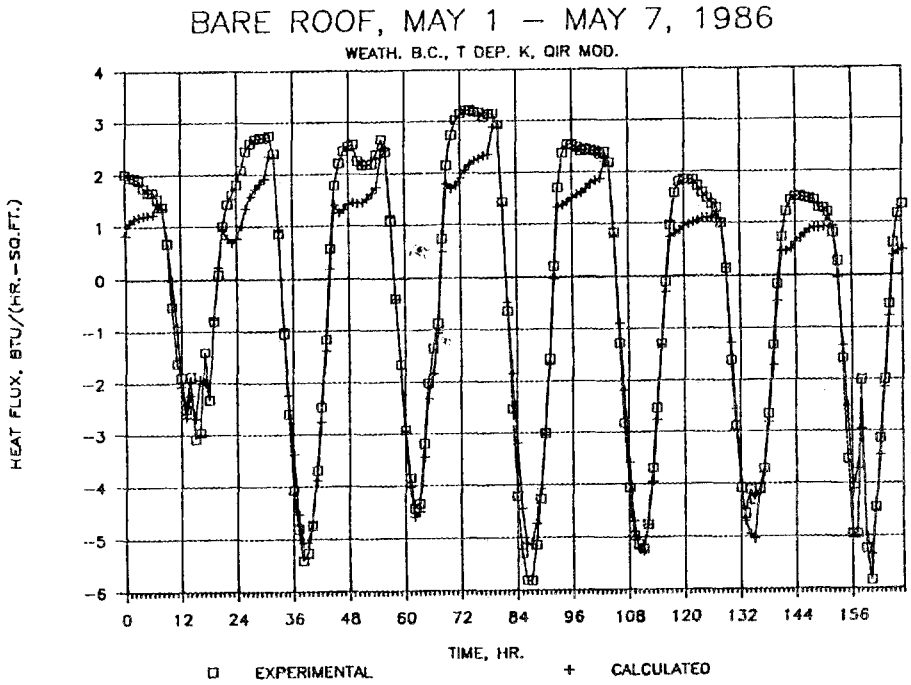

Fig. 3.24. Comparison of predicted and measured roof heat fluxes for bare roof in warm weather with weather boundary conditions, using temperature-dependent insulation thermal conductivity, modified infrared radiation, and solar absorptance of 0.7.

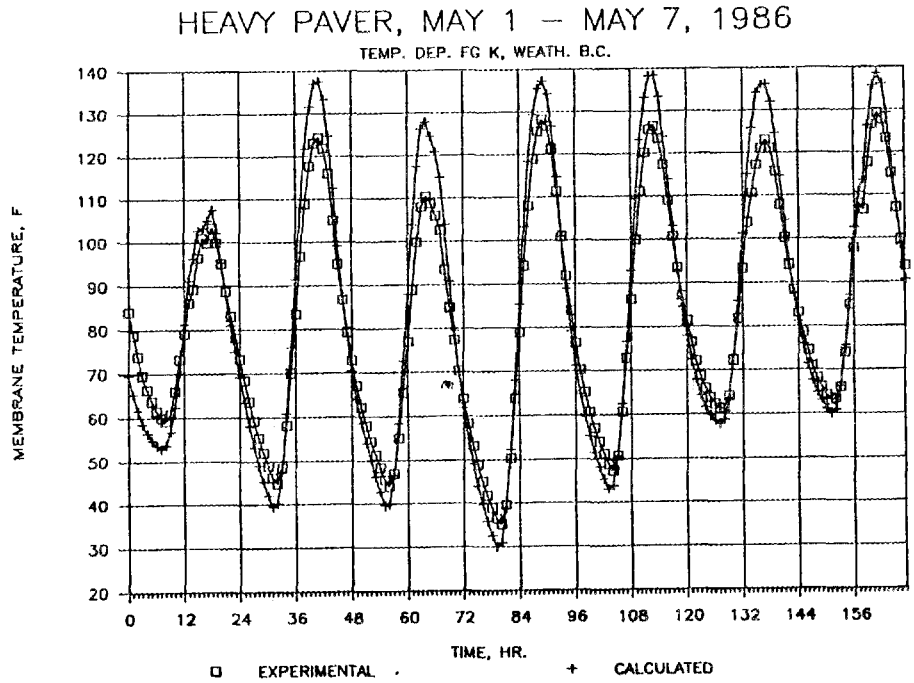

Fig. 3.25. Comparison of predicted and measured membrane temperatures for paver roof in warm weather with weather boundary conditions, using temperature-dependent insulation thermal conductivity.

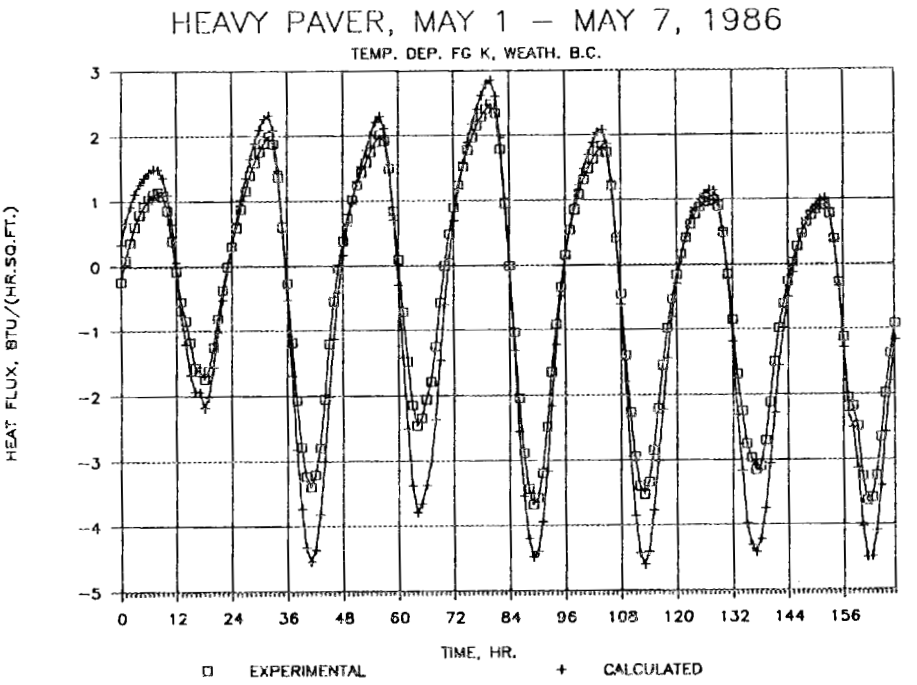

Fig. 3.26. Comparison of predicted and measured roof heat fluxes for paver roof in warm weather with weather boundary conditions, using temperature-dependent insulation thermal conductivity.

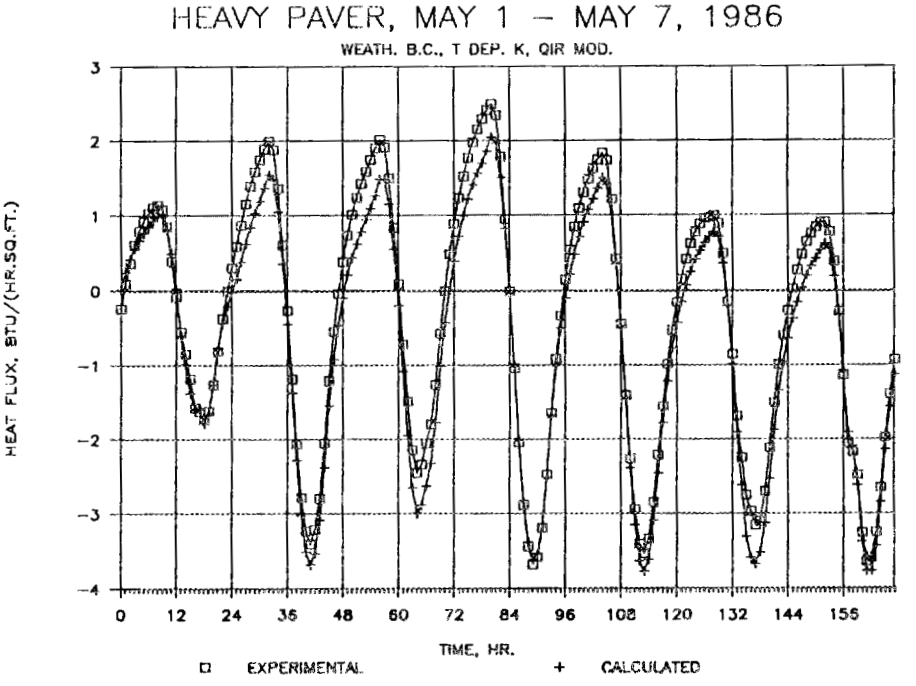

Fig. 3.27. Comparison of predicted and measured roof heat fluxes for paver roof in warm weather with weather boundary conditions, using temperature-dependent insulation thermal conductivity, modified infrared radiation and solar absorptance of 0.7.

Table 3.2. Comparison of predicted and measured peak membrane temperatures and weekly heat flows.

Roof	Period	Peak Temperature, °F Measured	Peak Temperature, °F Predicted	Positive Q* Measured	Positive Q* Predicted	Negative Q* Measured	Negative Q* Predicted
Bare	January	116	117	275	302	38	36
Bare	May	162	166	178	194	225	269
Paver	January	87	88	238	262	7	7
Paver	May	129	138	90	102	154	210

Note: Predictions made using weather boundary conditions and temperature-dependent insulation thermal conductivity.

* Weekly heat flows are in units of Btu/ft^2.

the negative heat flows for the week in May. Figures 3.24 and 3.27 showed that the use of a solar absorptance of 0.7 could improve the predictions. Using this solar absorptance, weekly negative heat flows would be 219 Btu/ft^2 for the bare roof and 173 Btu/ft^2 for the paver roof, which are significantly closer to the measured values than those calculated using the nominal solar absorptance of 0.84.

From the visual comparisons of predicted and measured membrane temperatures and heat flows and from the comparison of predicted and measured peak temperatures and weekly heat flows given in Table 3.2, it is concluded that the models capture the most important features of the diurnal cycles, the trends in weather during the weekly periods, and major differences between the weather conditions in the two weeks. It also appears that significant improvements can be obtained with refinements in the values for incident infrared radiation, and also possibly in the values that are used for solar absorptances and convection heat transfer coefficients.

4. SUMMARY AND CONCLUSIONS

An easy to use and computationally efficient computer model for the thermal performance of roofs has been developed and implemented on a personal computer. The model applies to one-dimensional transient heat conduction through multilayer roof systems and includes full coupling to ambient weather conditions. The model has been verified by comparing its predictions against experimental data taken at the Roof Thermal Research Apparatus. The experimental data were obtained during a cool week in January and February and during a warm week in May. The data were obtained on a roof section insulated with fiberglass insulation and covered with a modified bitumen membrane and on a similar roof section with a layer of concrete pavers added on top.

From visual inspections of plots of membrane temperature and roof heat flow, the model is judged to work very well when the boundary temperatures are known. It also is judged to work reasonably well when the ambient weather data are used as a boundary condition. The models capture the most important features of the diurnal cycles, the trends in weather during the weekly periods, and major differences between the weather conditions in the two weeks. It appears that significant improvements can be obtained with refinements in the values for incident infrared radiation, and also possibly in the values that are used for solar absorptances and convection heat transfer coefficients.

In its present form, the model is useful for predicting temperature profiles and heat flows through the large fraction of a roof that may be considered to be one-dimensional. However, it is not applicable to prediction of multidimensional effects such as those caused by penetrations, thermal bridges, and air gaps between insulation boards. Also, since the model is presently limited to heat conduction within the roof system, it does not account for the effects of moisture migration through wet roof systems, or for radiation and convection across air spaces between layers of the roof. Finally, the

model requires accurate values for material properties and weather parameters as inputs. Areas of applicability of the model will be expanded in future versions.

REFERENCES

1. G. E. Courville and J. V. Beck, "Techniques for in situ Determination of Thermal Resistance of Light Weight Board Insulation," Heat Transfer in Buildings and Structures, T. H. Kuehn and C. E. Hickox, editors, ASME HTD-Vol. 78, pp. 7-15 (1987).

2. J. V. Beck and K. J. Arnold, Parameter Estimation in Engineering and Science, New York, J. Wiley (1977).

3. S. V. Patankar, Numerical Heat Transfer and Fluid Flow, Hemisphere, New York (1980).

4. J. P. Holman, Heat Transfer, 5th Ed., pp. 191, 202, 272-286, McGraw-Hill, New York (1981).

5. J. Hilsenrath, H. J. Hoge, C. W. Beckett, J. F. Masi, W. S. Benedict, R. L. Nuttall, L. Fano, Y. S. Touloukian, and H. W. Woolley, "Tables of Thermodynamic and Transport Properties of Air, Argon, Carbon Dioxide, Carbon Monoxide, Hydrogen, Nitrogen, Oxygen, and Steam," NBS Circular 564, U. S. Dept. of Commerce (1960)

6. T. S. Chen, B. F. Armaly, and N. Ramachandran, "Correlations for Laminar Mixed Convection Flows on Vertical, Inclined, and Horizontal Flat Plates," ASME Journal of Heat Transfer, Vol. 108, pp. 835-840 (1986).

7. M. Martin and P. Berdahl, "Characteristics of Infrared Sky Radiation in the United States," Solar Energy, Vol. 33, pp. 321-336 (1984).

8. ASHRAE Handbook, 1985 Fundamentals, American Society of Heating, Refrigerating, and Air-Conditioning Engineers, Inc., Atlanta (1985).

9. NRCA Roofing Materials Guide, Volume 13, National Roofing Contractors Association, Rosemont, Illinois (August 1988).

APPENDIX A

STAR Computer Program

```
C*********************************************************************
C**                                                                 **
C**                        PROGRAM STAR                             **
C**                                                                 **
C**          (SIMPLIFIED TRANSIENT ANALYSIS OF ROOFS)               **
C*********************************************************************
C  THIS PROGRAM CALCULATES THE TRANSIENT HEAT TRANSFER ACROSS A
C  MULTILAYER ROOF STRUCTURE.  PROGRAM IS 1-DIMENSIONAL,
C  FINITE-DIFFERENCE, WITH EITHER EXPLICIT, IMPLICIT, OR
C  CRANK-NICOLSON FORMULATION.  TEMPERATURE DEPENDENT THERMAL
C  PROPERTIES ARE INCLUDED.
      DIMENSION N(20),L(20),NAME(20),KA(20),KB(20),CA(20),CB(20),
     & RHO(20),LI(20),X(2000),DLX(20),DX(2000),
     & A(2000),B(2000),C(2000),D(2000),T(2000),TO(2000),KT(2000),
     & CP(2000),DEN(2000),P(2000),Q(2000),T1(2000),TP(2000),QT(2000),
     & QI(21),TI(21),XT1(21),XT2(21)
      REAL KA,KB,L,LI,KT
      CHARACTER NAME*16
      DATA PI/3.14159265/,HFG/1060.0/
      OPEN(UNIT=9,FILE='OUT')
      WRITE(*,5)
    5 FORMAT(2X,'DO YOU WANT TO READ INPUT FROM SCREEN,',/,
     &       2X,'OR FROM AN INPUT FILE?',/,
     &       2X,'ENTER 0 FOR SCREEN, OR 1 FOR INPUT FILE',/)
      READ(*,*) IRUN
      IF(IRUN.EQ.1)  OPEN(UNIT=5,FILE='IN')
      IF(IRUN.EQ.0) WRITE(*,10)
   10 FORMAT(2X,'ENTER SLOPE OF ROOF,',/,
     & 2X,'INCHES RISE PER FOOT OF RUN',/)
      READ(5,*) SLOPE
      PHI = ATAN(SLOPE/12.0)*180.0/PI
      IF(IRUN.EQ.0) WRITE(*,20)
   20 FORMAT(2X,'ENTER LENGTH AND WIDTH OF ROOF, IN FEET',/)
      READ(5,*) ALEN,WID
C CALCULATE CHARACTERISTIC LENGTH FOR ROOF
      AL = (ALEN + WID)/2.0
      IF(IRUN.EQ.0) WRITE(*,30)
   30 FORMAT(2X,'ENTER NUMBER OF LAYERS IN ROOF, UP TO 20',/)
      READ(5,*) NLAYER
      IF(NLAYER.LT.1.OR.NLAYER.GT.20) STOP 'NLAYER MUST BE 1-20'
      IF(IRUN.EQ.0) WRITE(*,40)
   40 FORMAT(2X,'BEGIN INPUTTING DATA FOR EACH LAYER',/,
     & 2X,'STARTING AT THE OUTER SURFACE OF THE ROOF',/)
      DO 100 I = 1,NLAYER
      IF(IRUN.EQ.0) WRITE(*,50) I
   50 FORMAT(2X,'LAYER',1X,I3,1X,':',/)
      IF(IRUN.EQ.0) WRITE(*,51)
   51 FORMAT(2X,'ENTER NAME OF MATERIAL FOR LAYER',/)
      READ(5,52) NAME(I)
   52 FORMAT(A16)
      IF(IRUN.EQ.0) WRITE(*,55)
   55 FORMAT(2X,'ENTER THICKNESS OF LAYER, IN INCHES',/)
      READ(5,*) LI(I)
      IF(IRUN.EQ.0) WRITE(*,60)
```

```
 60 FORMAT(2X,'ENTER NUMBER OF NODES IN LAYER, LIMIT = 100',/)
    READ(5,*) N(I)
    AN = N(I)
    DLX(I) = LI(I)/12.0/AN
    IF(IRUN.EQ.0) WRITE(*,65)
 65 FORMAT(2X,'ENTER THERMAL CONDUCTIVITY OF LAYER',/,
   & 2X,'UNITS = BTU-IN/(HR-FT2-F)',/,
   & 2X,'CONSTANT VALUE, OR INTERCEPT FOR LINEAR WITH TEMP. = ?',/)
    READ(5,*) KA(I)
    IF(IRUN.EQ.0) WRITE(*,70)
 70 FORMAT(2X,'SLOPE FOR LINEAR WITH TEMP. = ?',/)
    READ(5,*) KB(I)
    IF(IRUN.EQ.0) WRITE(*,75)
 75 FORMAT(2X,'ENTER SPECIFIC HEAT OF LAYER',/,
   & 2X,'UNITS = BTU/(LB-F)',/,
   & 2X,'CONSTANT VALUE, OR INTERCEPT FOR LINEAR WITH TEMP. = ?',/)
    READ(5,*) CA(I)
    IF(IRUN.EQ.0) WRITE(*,70)
    READ(5,*) CB(I)
    IF(IRUN.EQ.0) WRITE(*,80)
 80 FORMAT(2X,'ENTER DENSITY OF LAYER, UNITS = PCF',/)
    READ(5,*) RHO(I)
100 CONTINUE
    IF(IRUN.EQ.0) WRITE(*,110)
110 FORMAT(2X,'ENTER INTEGER NUMBER OF CALCULATIONAL TIME',/,
   & 2X,'STEPS PER HOUR OF SIMULATED TIME',/)
    READ(5,*) NSTEP
    ANSTEP = NSTEP
    DT = 1.0/ANSTEP
    IF(IRUN.EQ.0) WRITE(*,120)
120 FORMAT(2X,'CHOOSE TRANSIENT SOLUTION TECHNIQUE:',/,
   & 6X,'0.0 = BACKWARDS EULER, OR EXPLICIT SCHEME',/,
   & 6X,'0.5 = CRANK-NICHOLSON SCHEME',/,
   & 6X,'1.0 = FULLY IMPLICIT SCHEME'/)
    READ(5,*) F
    IF(IRUN.EQ.0) WRITE(*,130)
130 FORMAT(2X,'SPECIFY TYPE OF BOUNDARY CONDITION ON OUTSIDE',/,
   & 2X,'0 = SPECIFIED TEMPERATURE',/,
   & 2X,'1 = WEATHER CONDITIONS',/)
    READ(5,*) IBCO
    IF(IBCO.EQ.1) OPEN(UNIT=8,FILE='WEA')
    IF(IBCO.EQ.0.OR.IBCI.EQ.0) OPEN(UNIT=10,FILE='EXP')
    IF(IBCO.EQ.0) GO TO 160
    IF(IRUN.EQ.0) WRITE(*,140)
140 FORMAT(2X,'ENTER SOLAR ABSORPTANCE AND IR EMITTANCE',/,
   & 2X,'OF OUTSIDE SURFACE',/)
    READ(5,*) AO,EO
    IF(IRUN.EQ.0) WRITE(*,142)
142 FORMAT(2X,'SPECIFY TYPE OF CONVECTION COEFF. AT OUTSIDE',/,
   & 2X,'0 = USER SPECIFIED HO',/,
   & 2X,'1 = CALCULATED FROM WEATHER AND CORRELATIONS',/)
    READ(5,*) IHO
    IF(IHO.EQ.1) GO TO 155
    IF(IRUN.EQ.0) WRITE(*,150)
```

```
  150 FORMAT(2X,'ENTER CONVECTION COEFFICIENT AT OUTSIDE',/,
     & 2X,'UNITS = BTU/(HR-FT2-F)',/)
      READ(5,*) HO
  155 IF(IRUN.EQ.0) WRITE(*,157)
  157 FORMAT(2X,'DO YOU WANT TO INCLUDE CONDENSATION AND',/,
     & 2X,'EVAPORATION OF MOISTURE AT OUTSIDE SURFACE?',/,
     & 2X,'0 = IGNORE',/,
     & 2X,'1 = INCLUDE',/)
      READ(5,*) ILAT
  160 CONTINUE
      IF(IRUN.EQ.0) WRITE(*,170)
  170 FORMAT(2X,'SPECIFY TYPE OF BOUNDARY CONDITION ON INSIDE',/,
     & 2X,'0 = SPECIFIED TEMPERATURE',/,
     & 2X,'1 = ROOM CONDITIONS',/)
      READ(5,*) IBCI
      IF(IBCI.EQ.0) GO TO 190
      IF(IRUN.EQ.0) WRITE(*,172)
  172 FORMAT(2X,'ENTER INDOOR TEMPERATURE, F',/)
      READ(5,*) TIN
      IF(IRUN.EQ.0) WRITE(*,175)
  175 FORMAT(2X,'SPECIFY TYPE OF CONVECTION COEFF. AT INSIDE',/,
     & 2X,'0 = USER SPECIFIED HI',/,
     & 2X,'1 = CALCULATED FROM CORRELATIONS',/)
      READ(5,*) IHI
      IF(IHI.EQ.1) GO TO 190
      IF(IRUN.EQ.0) WRITE(*,180)
  180 FORMAT(2X,'ENTER FILM COEFFICIENT ON INSIDE',/,
     & 2X,'UNITS = BTU/(HR-FT2-F)',/,
     & 2X,'CONVECTION PART ONLY',/)
      READ(5,*) HI
  190 CONTINUE
C  SET UP GRID, NODE NUMBERS START AT OUTER BOUNDARY
C  OTHER NODES ARE CENTERED WITHIN CONTROL VOLUMES
      I = 1
      X(1) = 0.0
      DX(1) = 0.0
      DO 200 J = 1,NLAYER
      I = I + 1
      DX(I) = DLX(J)
      DEN(I) = RHO(J)
      IF(J.EQ.1) X(I) = X(I-1) + DLX(J)/2.0
      IF(J.GT.1) X(I) = X(I-1) + DLX(J)/2.0 + DLX(J-1)/2.0
      M = N(J)
      DO 210 K = 2,M
      I = I + 1
      DX(I) = DLX(J)
      DEN(I) = RHO(J)
  210 X(I) = X(I-1) + DLX(J)
  200 CONTINUE
      I = I + 1
      X(I) = X(I-1) + DLX(NLAYER)/2.0
      DX(I) = 0.0
      NNODE = I
      WRITE(*,215)
```

```
  215 FORMAT(3X,'NODE',7X,'X',8X,'DX')
      DO 220 I = 1,NNODE
      WRITE(*,225) I,X(I),DX(I)
  225 FORMAT(2X,I5,2F10.4)
  220 CONTINUE
      PAUSE 'ENTER "RETURN" TO CONTINUE'
      WRITE(9,250) NLAYER+1
  250 FORMAT(8X,'TIME',5X,'WATER',5X,'T AND Q CALCULATED AT INTERFACES
     & 1 THROUGH',1X,I2)
C  INITIALIZE TEMPERATURES
      DO 300 I = 1,NNODE
      TO(I) = 75.0
      T(I) = 75.0
  300 T1(I) = 75.0
C  INITIALIZE MOISTURE ON OUTSIDE SURFACE
      WAT = 0.0
C  READ FIRST LINE OF INPUT DATA
      IF(IBCO.EQ.0.OR.IBCI.EQ.0) THEN
         READ(10,*)
         READ(10,*) TIME2,(XT1(I),I=1,NLAYER+1),QMEAS
         TBO1 = XT1(NLAYER+1)
         TBI1 = XT1(1)
      END IF
      IF(IBCO.EQ.1) THEN
         READ(8,*)
         READ(8,*) TIME1,TAIR1,HUM1,PBAR1,QSUN1,WS1,QIR1
      END IF
C  IF QIR > 0, QIR = INCIDENT INFRARED RADIATION
C  IF QIR < 0, QIR = CLOUD AMOUNT
      ITIME = 0
      IHR = 0
C  READ NEXT LINE OF INPUT DATA
  350 CONTINUE
      IF(IBCO.EQ.0.OR.IBCI.EQ.0)  THEN
          READ(10,*,END=999) TIME2,(XT2(I),I=1,NLAYER+1),QMEAS
          TBO2 = XT2(NLAYER+1)
          TBI2 = XT2(1)
      END IF
      IF(IBCO.EQ.1) THEN
          READ(8,*,END=999) TIME1,TAIR2,HUM2,PBAR2,QSUN2,WS2,QIR2
      END IF
      ITIME = ITIME + 1
      IHR = IHR + 1
      IF(IHR.GT.23) IHR = IHR - 24
      NN = 1
C  LOOP TO STEP THROUGH TIME STEPS WITHIN ONE SIMULATION PERIOD
  360 ANN = NN
      ANN = ANN/ANSTEP
      IF(IBCO.EQ.0.OR.IBCI.EQ.0) THEN
         TBO = TBO1 + ANN*(TBO2 - TBO1)
         TBI = TBI1 + ANN*(TBI2 - TBI1)
      END IF
      IF(IBCO.EQ.1) THEN
         TAIR = TAIR1 + ANN*(TAIR2 - TAIR1)
```

```
         QSUN = QSUN1 + ANN*(QSUN2 - QSUN1)
         HUM = HUM1 + ANN*(HUM2 - HUM1)
         PBAR = PBAR1 + ANN*(PBAR2 - PBAR1)
         WS = WS1 + ANN*(WS2 - WS1)
         QIR = QIR1 + ANN*(QIR2 - QIR1)
      END IF
      DO 365 I = 1,NNODE
  365 TO(I) = T(I)
C  CALCULATE THERMAL PROPERTIES FOR EACH NODE
C  AND START LOOP FOR TEMP. DEP. PROPERTIES
      NIT = 0
  370 NIT = NIT + 1
      DO 380  I = 1,NNODE
  380 T1(I) = T(I)
      I = 1
      DO 400 J = 1,NLAYER
      M = N(J)
      DO 400 K = 1,M
      I = I + 1
      IF(ABS(F-1.0).LT.1.E-3)  TP(I) = T1(I)
      IF(ABS(F-0.5).LT.1.E-3)  TP(I) = (T1(I) + TO(I))/2.0
      IF(ABS(F-0.0).LT.1.E-3)  TP(I) = TO(I)
      KT(I) = (KA(J) + KB(J)*TP(I))/12.0
      CP(I) = CA(J) + CB(J)*TP(I)
  400 CONTINUE
C  CHECK FOR CONVERGENCE CRITERION USING INITIAL PROPERTIES
      IF(ABS(F-1.0).LT.1.E-3) GO TO 490
      IF(ITIME.GT.1.OR.NN.GT.1.OR.NIT.GT.1)  GO TO 490
      DO 450 I = 2,NNODE-1
      ALF = KT(I)/CP(I)/DEN(I)
      AM = ALF*DT/DX(I)/DX(I)
      IF(AM.GT.0.5) THEN
      WRITE(*,460) I
  460 FORMAT(2X,'CONVERGENCE CRITERION FOR EXPLICIT METHOD',/,
     &       2X,'NOT SATISFIED AT INTERIOR NODE',2X,I5)
      IF(ABS(F).LT.1.E-3) STOP 'RUN TERMINATED WITH EXPLICIT METHOD'
      ELSE IF(AM.GT.0.25) THEN
      WRITE(*,461) I
  461 FORMAT(2X,'WARNING: CONVERGENCE CRITERION FOR EXPLICIT METHOD',/,
     &       2X,'NEAR LIMIT AT INTERIOR NODE',2X,I5)
      ELSE
      CONTINUE
      END IF
  450 CONTINUE
      PAUSE 'ENTER "RETURN" TO CONTINUE'
  490 CONTINUE
C  CALCULATE MATRIX COEFFICIENTS, SEE PATANKAR PP. XX-XX
      IF(IBCO.NE.0) THEN
        V = WS*5280.0
        IF(QIR.LE.0.0) THEN
           CLDAMT = - QIR
           CALL SKY(TAIR,HUM,IHR,CLDAMT,2,TSURR)
        ELSE
           TSURR = (QIR/1.714E-9)**0.25 - 459.67
```

```
      END IF
      HR = EO*1.714E-3*
     &     ((T1(1)+459.67)/100.*(T1(1)+459.67)/100.
     &    + (TSURR+459.67)/100.*(TSURR+459.67)/100.)*
     &     (T1(1) + TSURR + 2.0*459.67)/100.
      IF(IHO.EQ.1) CALL HCON(T1(1),TAIR,PHI,AL,1,V,HO)
      IF(ILAT.NE.0) THEN
        CALL HMASS(T1(1),TAIR,HO,HM)
        CALL PSY1(TAIR,HUM,PAIR,WAIR,DWADT)
        CALL PSY1(T1(1),100.0,PSURF,WSURF,DWSDT)
        AMW = HM*(WAIR - WSURF)
        IF(WAT.LE.1.E-8.AND.AMW.LT.0.0) THEN
             AMW = 0.0
             HM = 0.0
        ELSE IF(WAT.GT.0.0.AND.AMW.LT.0.0.AND.
     &       ABS(AMW*DT).GT.ABS(WAT))  THEN
             AMW = -WAT/DT
             HM = AMW/(WAIR - WSURF)
        ELSE
             CONTINUE
        END IF
      QLAT = AMW*HFG + HFG*HM*DWSDT*T1(1)
      ELSE
        AMW = 0.0
        QLAT = 0.0
      END IF
    A(1) = 0.0
    B(1) = 2.0*KT(2)/DX(2) + HO + HR
    IF(ILAT.NE.0) B(1) = B(1) + HFG*HM*DWSDT
    C(1) = -2.0*KT(2)/DX(2)
    D(1) = HR*TSURR + HO*TAIR + AO*QSUN + QLAT
    ELSE
    A(1) = 0.0
    B(1) = 1.0
    C(1) = 0.0
    D(1) = TBO
    END IF
    A(2) = -F*2.0*KT(2)/DX(2)
    B(2) = F*2.0*KT(2)/DX(2) + F*2.0/(DX(2)/KT(2) + DX(3)/KT(3))
   &       +DEN(2)*CP(2)*DX(2)/DT
    C(2) = -F*2.0/(DX(2)/KT(2) + DX(3)/KT(3))
    D(2) = DEN(2)*CP(2)*DX(2)/DT*TO(2) + (1.0 - F)*
   & ((TO(1)-TO(2))*2.0*KT(2)/DX(2)
   & -(TO(2)-TO(3))*2.0/(DX(2)/KT(2) + DX(3)/KT(3)))
    DO 500 I = 3,NNODE-2
    A(I) = -F*2.0/(DX(I)/KT(I) + DX(I-1)/KT(I-1))
    B(I) = F*2.0/(DX(I)/KT(I) + DX(I-1)/KT(I-1))
   &      +F*2.0/(DX(I)/KT(I) + DX(I+1)/KT(I+1))
   &      + DEN(I)*CP(I)*DX(I)/DT
    C(I) = -F*2.0/(DX(I)/KT(I) + DX(I+1)/KT(I+1))
    D(I) = DEN(I)*CP(I)*DX(I)/DT*TO(I) + (1.0 - F)*
   & ((TO(I-1)-TO(I))*2.0/(DX(I)/KT(I) + DX(I-1)/KT(I-1))
   & -(TO(I)-TO(I+1))*2.0/(DX(I)/KT(I) + DX(I+1)/KT(I+1)))
500 CONTINUE
```

```
      I = NNODE - 1
      A(I) = -F*2.0/(DX(I)/KT(I) + DX(I-1)/KT(I-1))
      B(I) = F*2.0/(DX(I)/KT(I) + DX(I-1)/KT(I-1))
     &      +F*2.0/(DX(I)/KT(I))
     &      + DEN(I)*CP(I)*DX(I)/DT
      C(I) = -F*2.0/(DX(I)/KT(I))
      D(I) = DEN(I)*CP(I)*DX(I)/DT*TO(I) + (1.0 - F)*
     & ((TO(I-1)-TO(I))*2.0/(DX(I)/KT(I) + DX(I-1)/KT(I-1))
     & -(TO(I)-TO(I+1))*2.0/(DX(I)/KT(I)))
      I = NNODE
      IF(IBCI.NE.0) THEN
      HRI = 0.9*1.714E-3*
     &       ((T1(NNODE)+459.67)/100.*(T1(NNODE)+459.67)/100.
     &      + (TIN+459.67)/100.*(TIN+459.67)/100.)*
     &       (T1(NNODE) + TIN + 2.0*459.67)/100.
      IF(IHI.EQ.1) CALL HCON(T1(NNODE),TIN,PHI,AL,2,0.0,HI)
      A(I) = -2.0*KT(I-1)/DX(I-1)
      B(I) = 2.0*KT(I-1)/DX(I-1) + HI + HRI
      C(I) = 0.0
      D(I) =  HI*TIN + HRI*TIN
      ELSE
      A(I) = 0.0
      B(I) = 1.0
      C(I) = 0.0
      D(I) = TBI
      END IF
C  SOLVE EXPLICIT EQUATIONS
      IF(ABS(F).LT.1.E-3)  THEN
      DO 550 I = 2,NNODE-1
  550 T(I) = D(I)/B(I)
      T(1) = (D(1) - C(1)*T(2))/B(1)
      T(NNODE) = (D(NNODE) - A(NNODE)*T(NNODE-1))/B(NNODE)
      ELSE
C  SOLVE TRIDIAGONAL MATRIX
      DO 600 I = 1,NNODE
      IF(I.EQ.1) P(I) = -C(I)/B(I)
      IF(I.NE.1) P(I) = -C(I)/(A(I)*P(I-1)+B(I))
      IF(I.EQ.1) Q(I) = D(I)/B(I)
  600 IF(I.NE.1) Q(I) = (-A(I)*Q(I-1) + D(I))/(A(I)*P(I-1) + B(I))
      T(NNODE) = Q(NNODE)
      DO 700 I = 1,NNODE-1
      K = NNODE - I
      T(K) = P(K)*T(K+1) + Q(K)
  700 CONTINUE
      END IF
C  CHECK FOR CONVERGENCE FOR TEMPERATURE DEPENDENT PROPERTIES
      IF(ABS(F).LT.1.E-3.AND.ILAT.EQ.0.AND.IBCO.EQ.0) GO TO 760
      DO 750 I = 1,NNODE
      IF(ABS(T(I)-T1(I)).GT.1.E-3.AND.NIT.LE.10)  GO TO 370
  750 CONTINUE
  760 CONTINUE
C  INCREMENT TIME STEP AND REPEAT
      WAT = WAT + AMW*DT
      NN = NN + 1
```

```
      IF (NN.LE.NSTEP) GO TO 360
C  CALCULATE HEAT FLUXES AT NODES
      QT(1) = -2.0*KT(2)*(T(1)-T(2))/DX(2)
      QT(2) = -KT(2)*(T(1)-T(2))/DX(2)
     &       - (T(2)-T(3))/(DX(2)/KT(2) + DX(3)/KT(3))
      QT(NNODE-1) = -(T(NNODE-2)-T(NNODE-1))/(DX(NNODE-2)/KT(NNODE-2)
     &                                     + DX(NNODE-1)/KT(NNODE-1))
     &              -(T(NNODE-1)-T(NNODE))/(DX(NNODE-1)/KT(NNODE-1))
      QT(NNODE)=-2.0*KT(NNODE-1)*(T(NNODE-1)-T(NNODE))/DX(NNODE-1)
      DO 800 I = 3,NNODE-2
      QT(I) = -(T(I-1)-T(I))/(DX(I-1)/KT(I-1) + DX(I)/KT(I))
     &       -(T(I)-T(I+1))/(DX(I)/KT(I) + DX(I+1)/KT(I+1))
  800 CONTINUE
C  CALCULATE HEAT FLUXES AND TEMPERATURES AT INTERFACES
      QI(1) = QT(1)
      TI(1) = T(1)
      M = 1
      DO 900 J = 1,NLAYER-1
      M = M + N(J)
      QI(J+1) = -2.0*(T(M)-T(M+1))/(DX(M)/KT(M) + DX(M+1)/KT(M+1))
      TI(J+1) = T(M) + QI(J+1)*DX(M)/2.0/KT(M)
  900 CONTINUE
      QI(NLAYER+1) = QT(NNODE)
      TI(NLAYER+1) = T(NNODE)
C  WRITE OUT RESULTS
      WRITE(9,1000) ITIME,WAT,(TI(I),QI(I),I=1,NLAYER+1)
 1000 FORMAT(2X,I10,F10.4,21(F10.2,F10.4))
      WRITE(*,1001) ITIME
 1001 FORMAT(1X,'CALCULATIONS FINISHED FOR HOUR',5X,I5)
      IF(IBCO.EQ.0.OR.IBCI.EQ.0) THEN
        TBO1 = TBO2
        TBI1 = TBI2
      END IF
      IF(IBCO.EQ.1) THEN
        TAIR1 = TAIR2
        QSUN1 = QSUN2
        HUM1 = HUM2
        PBAR1 = PBAR2
        WS1 = WS2
        QIR1 = QIR2
      END IF
      GO TO 350
  999 STOP  'CALCULATIONS COMPLETED'
      END
C***********************************************************************
C**                                                                   **
C**                          SUBROUTINE HCON                          **
C**                                                                   **
C***********************************************************************
      SUBROUTINE HCON(TS,TA,PHI,AL,IFLAG,V,HC)
C  THIS SUBROUTINE CALCULATES NATURAL CONVECTION HEAT TRANSFER
C  COEFFICIENTS BASED ON ISOLATED ISOTHERMAL FLAT PLATES
C  CALCULATES FORCED CONVECTION COEFFICIENTS AND TOTAL
C  CONVECTION HEAT TRANSFER COEFFICIENTS
```

```
C  SEE HOLMAN, 5TH EDITION, PP. 272-286
C  TS = SURFACE TEMPERATURE, F
C  TA = AIR TEMPERATURE, F
C  PHI = TILT ANGLE, DEGREES, 0 FOR HORIZONTAL, 90 FOR VERTICAL
C  AL = CHARACTERISTIC LENGTH OF SURFACE
C  IFLAG = 1 FOR SURFACE FACING UPWARD
C  IFLAG = 2 FOR SURFACE FACING DOWNWARD
C  V = AIR SPEED, FEET PER HOUR
C  HCF = FORCED CONVECTION COEFFICIENT
C  HCN = NATURAL CONVECTION COEFFICIENT
C  HC = TOTAL CONVECTION COEFFICIENT
C
      REAL NUS,K,MU,NU
      DT = TS - TA
      IF (IFLAG.EQ.2)  DT = -DT
C  CALCULATE FILM TEMPERATURE
      TF = (TS+TA)/2.0
      TF1 = TF
      IF(ABS(PHI).GT.1.E-3.AND.ABS(PHI-90.).GT.1.E-3)
     1    TF = TS - 0.25*(TS-TA)
      IF(ABS(PHI).GT.1.E-3.AND.ABS(PHI-90.).GT.1.E-3)
     1    TF1 = TA + 0.25*(TS-TA)
      TK = (TF+459.67)/1.8
C  THERMAL CONDUCTIVITY OF AIR FROM EQUATION IN NBS CIRC. 564
C  THERMAL COND. IN BTU/(HR-FT-F)
      K = 0.6325E-5*SQRT(TK)/(1.+(245.4*10.**(-12./TK))/TK)*241.77
C  DYNAMIC VISCOSITY OF AIR FROM EQUATION IN NBS CIRC. 564
C  LB/(HR-FT)
      MU = (145.8*TK*SQRT(TK)/(TK+110.4))*241.90E-7
C  PRANDTL NUMBER, LINEAR REGRESSION FROM 220 K TO 360 K
C  FROM NBS CIRC. 564
      PR = 0.7880 - 2.631E-4*TK
C  VOLUME EXPANSION COEFFICIENT OF AIR, 1/TABS, PERFECT GAS
      BETA = 1./(TF1+459.67)
C  DENSITY OF AIR, PERFECT GAS, NBS CIRC. 564, LB/CF
      RHO = 22.0493/TK
C  KINEMATIC VISCOSITY, FT2/HR
      NU = MU/RHO
C  SPECIFIC HEAT OF AIR, LINEAR REGRESSION FROM 220 K TO 360 K
C  FROM NBS CIRC. 564, BTU/(LB-F)
      CP = (3.4763 + 1.066E-4*TK)*0.068559
C  RAYLEIGH NUMBER, LEADING COEFFICIENT IS
C  32.174*3600*3600, FT/HR2
      RA = (4.16975E8)*BETA*RHO*CP*ABS(DT)*(AL**3)/NU/K
C  BRANCH TO DIFFERENT CORRELATIONS DEPENDING UPON
C  SURFACE ORIENTATION
      IF(ABS(PHI).LE.1.E-3)  GO TO 100
      IF(ABS(PHI-90.).LE.1.E-3)  GO TO 200
      IF(ABS(PHI).GT.1.E-3.AND.ABS(PHI).LT.2.)  GO TO 300
      IF(ABS(PHI).GT.2.0.AND.ABS(PHI-90.).GT.1.E-3)  GO TO 400
C  FOR HORIZONTAL SURFACES
  100 IF(DT.LT.0.0)  GO TO 150
      NUS = 0.15*RA**(1./3.)
      IF(RA.LT.8.E6)  NUS = 0.54*RA**0.25
```

```
      GO TO 1000
  150 NUS = 0.58*RA**0.2
      GO TO 1000
C  FOR VERTICAL SURFACES
  200 NUS = 0.10*RA**(1./3.)
      IF(RA.LT.1.E9)  NUS = 0.59*RA**0.25
      GO TO 1000
C  FOR NEARLY HORIZONTAL(UP TO 2 DEGREES TILT) SURFACES
  300 IF(DT.GT.0.0)  GO TO 450
      NUS = 0.58*RA**0.2
      GO TO 1000
C  FOR TILTED SURFACES
  400 IF(DT.GT.0.0)  GO TO 450
      NUS = 0.56*(RA*COS((90.-PHI)*3.14159265/180.))**0.25
      GO TO 1000
  450 GRC = 10.0**(PHI/(1.1870+0.0870*PHI))
      IF(ABS(PHI).LT.15.)  GRC = 1.E6
      IF(ABS(PHI).GT.75.)  GRC = 5.E9
      GR = RA/PR
      IF(GR.LE.GRC)  NUS=0.56*(RA*COS((90.-PHI)*3.14159265/180.))**0.25
      IF(GR.GT.GRC)  NUS = 0.14*(RA**(1./3.) - (GRC*PR)**(1./3.))
     1   +0.56*(GRC*PR*COS((90.-PHI)*3.14159265/180.))**0.25
      GO TO 1000
 1000 HCN = NUS*K/AL
C  CALCULATE FORCED CONVECTION COEFFICIENT
C  SEE HOLMAN, 5TH EDITION, PG. 191, EQN. 5-44, 5-46
C  AND PG. 202, EQN. 5-85
      RE = V*AL/NU
      IF(RE.LT.5.E5)  NUS = 0.664*(PR**(1./3.))*SQRT(RE)
      IF(RE.GT.5.E5)  NUS = (PR**(1./3.))*(0.037*(RE**0.8)-850.)
      HCF = NUS*K/AL
C  COMBINE NATURAL AND FORCED CONVECTION COEFFICIENTS
C  USING CHURCHILL'S CORRELATION
C  SEE J. HEAT TRANS., VOL. 108, PP. 835-840 (1986)
C  ASSUME ASSISTING FLOW IN ALL CASES
      HC = (HCF**3 + HCN**3)**(1./3.)
      RETURN
      END
C*********************************************************************
C**                                                                 **
C**                        SUBROUTINE HMASS                         **
C**                                                                 **
C*********************************************************************
      SUBROUTINE HMASS(TS,TA,HC,HM)
C  THIS SUBROUTINE CALCULATES THE MASS TRANSFER COEFFICIENT FOR
C  MOISTURE TRANSFER BETWEEN A SURFACE AND MOIST AIR
C  USING THE LEWIS RELATIONSHIP, AND EVALUATING ALL THERMOPHYSICAL
C  PROPERTIES AS THOSE OF DRY AIR
C  SEE HOLMAN, 5TH EDITION, PP. 494
C  TS = SURFACE TEMPERATURE, F
C  TA = AIR TEMPERATURE, F
C  HC = CONVECTION HEAT TRANSFER COEFFICIENT
C  HM = MASS TRANSFER COEFFICIENT, LB/(HR-FT2)
C
```

```
      REAL K
C  CALCULATE FILM TEMPERATURE
      TF = (TS+TA)/2.0
      TK = (TF+459.67)/1.8
C  THERMAL CONDUCTIVITY OF AIR FROM EQUATION IN NBS CIRC. 564
C  THERMAL COND. IN BTU/(HR-FT-F)
      K = 0.6325E-5*SQRT(TK)/(1.+(245.4*10.**(-12./TK))/TK)*241.77
C  DENSITY OF AIR, PERFECT GAS, NBS CIRC. 564, LB/CF
      RHO = 22.0493/TK
C  SPECIFIC HEAT OF AIR, LINEAR REGRESSION FROM 220 K TO 360 K
C  FROM NBS CIRC. 564, BTU/(LB-F)
      CP = (3.4763 + 1.066E-4*TK)*0.068559
C  CALCULATE THERMAL DIFFUSIVITY, FT2/HR
      ALF = K/CP/RHO
C  CALCULATE DIFFUSION COEFFICIENT FOR WATER VAPOR THROUGH AIR
C  D = FT2/HR, SEE 1985 ASHRAE HANDBOOK, PG. 5.2
      D = 0.035883/101.32*(TK**2.5)/(TK+245.0)
      HM = HC/CP/((ALF/D)**(2.0/3.0))
      RETURN
      END
C*********************************************************************
C**                                                                 **
C**                          SUBROUTINE PSY1                        **
C**                                                                 **
C*********************************************************************
      SUBROUTINE PSY1(T,HUM,P,W,DWSDT)
C  THIS SUBROUTINE CALCULATES THE WATER VAPOR PARTIAL PRESSURE AND
C  THE HUMIDITY RATIO, GIVEN THE TEMPERATURE AND RELATIVE HUMIDITY
C  USING EQUATION FROM 1985 ASHRAE FUNDAMENTALS P.6.6
C  T = DRYBULB TEMPERATURE, DEGREES F
C  HUM = RELATIVE HUMIDITY, PERCENT
C  P = WATER VAPOR PARTIAL PRESSURE, PSIA
C  W = HUMIDITY RATIO, POUNDS OF WATER PER POUNDS OF DRY AIR
      C1 = -10214.16
      C2 = -4.8932631
      C3 = -0.53769056E-2
      C4 = 0.19202377E-6
      C5 = 0.35575832E-9
      C6 = 0.090344688E-12
      C7 = 4.1635019
      C8 = -10440.4
      C9 = -11.2946669
      C10 = -0.02700133
      C11 = 0.12897060E-4
      C12 = -0.2478068E-8
      C13 = 6.5459673
      TR = T + 459.67
      IF(T.GE.32.0)  GO TO 10
      X = C1/TR + C2 + C3*TR + C4*TR*TR +C5*TR**3+C6*TR**4+C7*ALOG(TR)
      DXDT = -C1/TR/TR + C3 + 2.0*C4*TR + 3.0*C5*TR*TR + 4.0*C6*TR**3
     &       + C7/TR
      GO TO 20
   10 X = C8/TR + C9 + C10*TR + C11*TR*TR + C12*TR**3 + C13*ALOG(TR)
      DXDT = -C8/TR/TR + C10 + 2.0*C11*TR + 3.0*C12*TR*TR + C13/TR
```

```
   20 PSAT = EXP(X)
      DPSDT = PSAT*DXDT
      P = (HUM/100.0)*PSAT
      W = 0.62198*P/(14.696-P)
      DWSDT = 14.696*0.62198/(14.696-PSAT)/(14.696-PSAT)*DPSDT
      RETURN
      END
C*********************************************************************
C**                                                                 **
C**                          SUBROUTINE SKY                         **
C**                                                                 **
C*********************************************************************
      SUBROUTINE SKY(TO,HUM,IHR,CLDAMT,ICLDTY,TS)
      CALL PSY1(TO,HUM,P,W,DWSDT)
      ALF = ALOG(P*29.921/14.696)
      IF(P.GT.0.08865) TDP = 79.047 + 30.5790*ALF + 1.8893*ALF*ALF
      IF(P.LE.0.08865) TDP = 71.98 + 24.873*ALF + 0.8927*ALF*ALF
      TD = (TDP+459.67)/1.8 - 273.15
      EPS = 0.711 + 0.56*TD/100. + 0.73*(TD/100.)*(TD/100.) + 0.013*
     &  COS(2.0*3.14159265/24.*FLOAT(IHR))
      EPS = EPS + (1.0 - EPS)*CLDAMT/10.*0.784
      TS = (TO+459.67)*SQRT(SQRT(EPS)) - 459.67
      RETURN
      END
```

APPENDIX B

Basic Input for STAR Program (Interactive)

```
C:\FORTRM\ROOF>
C:\FORTRM\ROOF>SET WEA = MAY01PAV.PRN

C:\FORTRM\ROOF>SET OUT = PAV10.DAT

C:\FORTRM\ROOF>STAR

 DO YOU WANT TO READ INPUT FROM SCREEN,
 OR FROM AN INPUT FILE?
 ENTER 0 FOR SCREEN, OR 1 FOR INPUT FILE
0

 ENTER SLOPE OF ROOF,
 INCHES RISE PER FOOT OF RUN
0.0

 ENTER LENGTH AND WIDTH OF ROOF, IN FEET
4.0,4.0

 ENTER NUMBER OF LAYERS IN ROOF, UP TO 20
7

 BEGIN INPUTTING DATA FOR EACH LAYER
 STARTING AT THE OUTER SURFACE OF THE ROOF

 LAYER   1 :

 ENTER NAME OF MATERIAL FOR LAYER
BIT

 ENTER THICKNESS OF LAYER, IN INCHES
0.160

 ENTER NUMBER OF NODES IN LAYER, LIMIT = 100
1

 ENTER THERMAL CONDUCTIVITY OF LAYER
 UNITS = BTU-IN/(HR-FT2-F)
 CONSTANT VALUE, OR INTERCEPT FOR LINEAR WITH TEMP. = ?
1.14

 SLOPE FOR LINEAR WITH TEMP. = ?
0.0

 ENTER SPECIFIC HEAT OF LAYER
 UNITS = BTU/(LB-F)
 CONSTANT VALUE, OR INTERCEPT FOR LINEAR WITH TEMP. = ?
0.35

 SLOPE FOR LINEAR WITH TEMP. = ?
0.0

 ENTER DENSITY OF LAYER, UNITS = PCF
67.5
```

```
 LAYER   2 :

 ENTER NAME OF MATERIAL FOR LAYER
PAV

 ENTER THICKNESS OF LAYER, IN INCHES
1.8750

 ENTER NUMBER OF NODES IN LAYER, LIMIT = 100
4

 ENTER THERMAL CONDUCTIVITY OF LAYER
 UNITS = BTU-IN/(HR-FT2-F)
 CONSTANT VALUE, OR INTERCEPT FOR LINEAR WITH TEMP. = ?
12.0

 SLOPE FOR LINEAR WITH TEMP. = ?
0.0

 ENTER SPECIFIC HEAT OF LAYER
 UNITS = BTU/(LB-F)
 CONSTANT VALUE, OR INTERCEPT FOR LINEAR WITH TEMP. = ?
0.220

 SLOPE FOR LINEAR WITH TEMP. = ?
0.0

 ENTER DENSITY OF LAYER, UNITS = PCF
140.0

 LAYER   3 :

 ENTER NAME OF MATERIAL FOR LAYER
BIT

 ENTER THICKNESS OF LAYER, IN INCHES
0.2225

 ENTER NUMBER OF NODES IN LAYER, LIMIT = 100
1

 ENTER THERMAL CONDUCTIVITY OF LAYER
 UNITS = BTU-IN/(HR-FT2-F)
 CONSTANT VALUE, OR INTERCEPT FOR LINEAR WITH TEMP. = ?
1.14

 SLOPE FOR LINEAR WITH TEMP. = ?
0.0

 ENTER SPECIFIC HEAT OF LAYER
 UNITS = BTU/(LB-F)
 CONSTANT VALUE, OR INTERCEPT FOR LINEAR WITH TEMP. = ?
0.35
```

```
 SLOPE FOR LINEAR WITH TEMP. = ?
0.0

 ENTER DENSITY OF LAYER, UNITS = PCF
67.5

 LAYER   4 :

 ENTER NAME OF MATERIAL FOR LAYER
FG

 ENTER THICKNESS OF LAYER, IN INCHES
0.9375

 ENTER NUMBER OF NODES IN LAYER, LIMIT = 100
2

 ENTER THERMAL CONDUCTIVITY OF LAYER
 UNITS = BTU-IN/(HR-FT2-F)
 CONSTANT VALUE, OR INTERCEPT FOR LINEAR WITH TEMP. = ?
0.20525

 SLOPE FOR LINEAR WITH TEMP. = ?
0.00065

 ENTER SPECIFIC HEAT OF LAYER
 UNITS = BTU/(LB-F)
 CONSTANT VALUE, OR INTERCEPT FOR LINEAR WITH TEMP. = ?
0.23

 SLOPE FOR LINEAR WITH TEMP. = ?
0.0

 ENTER DENSITY OF LAYER, UNITS = PCF
13.2

 LAYER   5 :

 ENTER NAME OF MATERIAL FOR LAYER
FG

 ENTER THICKNESS OF LAYER, IN INCHES
0.9375

 ENTER NUMBER OF NODES IN LAYER, LIMIT = 100
2

 ENTER THERMAL CONDUCTIVITY OF LAYER
 UNITS = BTU-IN/(HR-FT2-F)
 CONSTANT VALUE, OR INTERCEPT FOR LINEAR WITH TEMP. = ?
0.20525

 SLOPE FOR LINEAR WITH TEMP. = ?
```

```
0.00065

 ENTER SPECIFIC HEAT OF LAYER
 UNITS = BTU/(LB-F)
 CONSTANT VALUE, OR INTERCEPT FOR LINEAR WITH TEMP. = ?
0.23

 SLOPE FOR LINEAR WITH TEMP. = ?
0.0

 ENTER DENSITY OF LAYER, UNITS = PCF
13.2

 LAYER   6 :

 ENTER NAME OF MATERIAL FOR LAYER
FG

 ENTER THICKNESS OF LAYER, IN INCHES
0.9375

 ENTER NUMBER OF NODES IN LAYER, LIMIT = 100
2

 ENTER THERMAL CONDUCTIVITY OF LAYER
 UNITS = BTU-IN/(HR-FT2-F)
 CONSTANT VALUE, OR INTERCEPT FOR LINEAR WITH TEMP. = ?
0.20525

 SLOPE FOR LINEAR WITH TEMP. = ?
0.00065

 ENTER SPECIFIC HEAT OF LAYER
 UNITS = BTU/(LB-F)
 CONSTANT VALUE, OR INTERCEPT FOR LINEAR WITH TEMP. = ?
0.23

 SLOPE FOR LINEAR WITH TEMP. = ?
0.0

 ENTER DENSITY OF LAYER, UNITS = PCF
13.2

 LAYER   7 :

 ENTER NAME OF MATERIAL FOR LAYER
FG

 ENTER THICKNESS OF LAYER, IN INCHES
0.9375

 ENTER NUMBER OF NODES IN LAYER, LIMIT = 100
2
```

```
 ENTER THERMAL CONDUCTIVITY OF LAYER
 UNITS = BTU-IN/(HR-FT2-F)
 CONSTANT VALUE, OR INTERCEPT FOR LINEAR WITH TEMP. = ?
0.20525

 SLOPE FOR LINEAR WITH TEMP. = ?
0.00065

 ENTER SPECIFIC HEAT OF LAYER
 UNITS = BTU/(LB-F)
 CONSTANT VALUE, OR INTERCEPT FOR LINEAR WITH TEMP. = ?
0.23

 SLOPE FOR LINEAR WITH TEMP. = ?
0.0

 ENTER DENSITY OF LAYER, UNITS = PCF
13.2

 ENTER INTEGER NUMBER OF CALCULATIONAL TIME
 STEPS PER HOUR OF SIMULATED TIME
10

 CHOOSE TRANSIENT SOLUTION TECHNIQUE:
     0.0 = BACKWARDS EULER, OR EXPLICIT SCHEME
     0.5 = CRANK-NICHOLSON SCHEME
     1.0 = FULLY IMPLICIT SCHEME
1.0

 SPECIFY TYPE OF BOUNDARY CONDITION ON OUTSIDE
 0 = SPECIFIED TEMPERATURE
 1 = WEATHER CONDITIONS
1

 ENTER SOLAR ABSORPTANCE AND IR EMITTANCE
 OF OUTSIDE SURFACE
0.84,0.9

 SPECIFY TYPE OF CONVECTION COEFF. AT OUTSIDE
 0 = USER SPECIFIED HO
 1 = CALCULATED FROM WEATHER AND CORRELATIONS
1

 DO YOU WANT TO INCLUDE CONDENSATION AND
 EVAPORATION OF MOISTURE AT OUTSIDE SURFACE?
 0 = IGNORE
 1 = INCLUDE
1


 SPECIFY TYPE OF BOUNDARY CONDITION ON INSIDE
 0 = SPECIFIED TEMPERATURE
 1 = ROOM CONDITIONS
0
```

APPENDIX C

Basic Input for STAR Program (External File)

```
        0.0
        4.0      4.0
          7
BIT
      0.160
          1
       1.14
        0.0
       0.35
        0.0
       67.5
PAV
     1.8750
          4
       12.0
        0.0
      0.220
        0.0
      140.0
BIT
      0.2225
          1
       1.14
        0.0
       0.35
        0.0
       67.5
FG
      0.9375
          2
     0.20525
     0.00065
        0.23
        0.0
       13.2
FG
      0.9375
          2
     0.20525
     0.00065
        0.23
        0.0
       13.2
FG
      0.9375
          2
     0.20525
     0.00065
        0.23
        0.0
       13.2
```

FG

0.9375	
2	
0.20525	
0.00065	
0.23	
0.0	
13.2	
10	
1.0	
1	
0.84	0.9
1	
1	
0	

INTERNAL DISTRIBUTION

1. R. S. Carlsmith
2. K. W. Childs
3. G. E. Courville
4. G. A. Dailey
5. W. Fulkerson
6. T. G. Kollie
7. M. A. Kuliasha
8. D. L. McElroy
9. H. A. McLain
10. W. R. Mixon
11. D. E. Reichle
12. C. J. Remenyik
13. E. Rogers
14-28. S. D. Samples
29. R. B. Shelton
30. V. J. Tennery
31. T. J. Wilbanks
32-41. K. E. Wilkes
42-44. Laboratory Records
45. Laboratory Records - RC
46. ORNL Patent Office
47. Y-12 Technical Library
48. Central Research Library
49. Document Reference Section

EXTERNAL DISTRIBUTION

50. F. Abel, Department of Energy, Washington, DC
51. R. L. Alumbaugh, Naval Civil Engineering Lab., Port Hueneme, CA
52. R. W. Anderson, 7090 Tecumseh Lane, Chanhassen, MN
53. G. Askew, 1120 Fieldstone Dr., Hixson, TN
54. E. Bales, New Jersey Institute of Technology, Newark, NJ
55. J. V. Beck, Michigan State University, East Lansing, MI
56. M. Bomberg, National Research Council of Canada, Ottawa, Ontario
57. W. C. Brown, National Research Council of Canada, Ottawa, Ontario
58. W. Carroll, Lawrence Berkeley Laboratory, Berkeley, CA
59. R. Coursey, J. P. Stevens & Company, North Hampton, MA
60. J. J. Cuttica, Gas Research Institute, Chicago, IL
61. B. J. Dempsey, 1205 Newmark C.E. Lab., Urbana, IL
62. A. Desjarlais, Thermatest Division of Holometrix, Inc., Cambridge, MA
63. D. M. Evans, Jr., Steven Winter Associates, Inc., New York, NY
64. T. A. Farkas, NAHB, Washington, DC
65. H. A. Fine, 949 Wishbone Circle, Lexington, KY
66. W. R. French, Moisture Systems, Inc., Houston, TX
67. L. R. Glicksman, MIT, Cambridge, MA
68. F. C. Gorham, Roofing Services, Inc., Springfield, VA
69. J. R. Hagan, Jim Walter Research, St. Petersburg, FL
70. D. A. Harris, NIBS, Washington, DC
71. J. Harris, Bonneville Power Administration, Portland, OR
72. R. O. Hinckley, University of Southwestern Louisiana, Lafayette, LA
73. B. Howard, NAHB National Research Center, Upper Marlboro, MD
74. J. L. Ius, Tyndall Air Force Base, FL
75. D. Johnson, Electra Manufacturing Corp., Holland, OH
76. J. P. Kalt, Harvard University, Cambridge, MA

77. M. Krarti, Steven Winter Associates, Inc., Norwalk, CT
78. M. B. Lacher, CertainTeed Corp., Valley Forge, PA
79. E. Leger, P.O. Box 549, New Boston, NH
80. M. D. Lyberg, SIB Box 785, Gavle, Sweden
81. R. Mack, Dow Chemical, Freeport, TX
82. P. C. Martin, Manville Sales Corp., Denver, CO
83. M. McBride, Owens-Corning Fiberglas, Granville, OH
84. D. McGuire, Regal Industries, Crothersville, IN
85. G. Miller, Jim Walter Research Corp., St. Petersburg, FL
86. M. Millspaugh, Reflectix, Inc., Markleville, IN
87. M. Modera, Lawrence Berkeley Laboratory, Berkeley, CA
88. R. L. Perrine, University of California, Los Angeles, CA
89. F. J. Powell, 9919 Mayfield Drive, Bethesda, MD
90. RSI Magazine, 7500 Old Oak Blvd., Cleveland, OH
91. B. K. Rabb, ACOUSTI Engineering of Alabama, Birmingham, AL
92. D. E. Richards, Owens-Corning Fiberglas, Toledo, OH
93. W. J. Rossiter, NIST, Gaithersburg, MD
94. J. A. Roux, University of Mississippi, University, MS
95. J. Samos, NASA - Langley, Hampton, VA
96. R. C. Schroter, Product Technical Service Associates, Orinda, CA
97. S. Selkowitz, Lawrence Berkeley Laboratory, Berkeley, CA
98. C. J. Shirtliffe, IRC/NRCC, Ottawa, Ontario
99. J. A. Smith, DOE/CE, Washington, DC
100. S. E. Smith, Holometrix, Inc., Cambridge, MA
101. M. K. Snyder, 9107 Outlook Drive, Overland Park, KS
102. L. G. Spielvogel, Wyncote House, Wyncote, PA
103. K. Spittle, The Spittle Co., Belmont, NC
104. R. Sterling, University of Minnesota, Minneapolis, MN
105. E. Story, Insultray, Oak Harbor, WA
106. R. Sullivan, National Center for Appropriate Technology, Butte, MT
107. A. TenWolde, U.S. Dept. of Agriculture, Forest Products Lab., Madison, WI
108. S. Tewes, SCH-BRC, Champaign, IL
109. S. Theimer, Librarian, CAREIRS/ASI, Arlington, VA
110. H. R. Trechsel, P.O. Box 211, Germantown, MD
111. G. A. Tsongas, Portland State University, Portland, OR
112. A. Tuluca, Steven Winter Associates, Norwalk, CT
113. R. P. Tye, Thermatest Division of Holometrix, Inc., Cambridge, MA
114. M. G. Van Geem, Construction Technology Laboratories, Inc. Skokie, IL
115. C. R. Vander Linden, Vander Linden & Associates, Littleton, CO
116. D. W. Yarbrough, Tenn. Tech. Univ., Cookeville, TN
117. Office of the Assistant Manager, Energy Research and Development, DOE/ORO, Oak Ridge, TN

118-127. Office of Scientific and Technical Information, U.S. Department of Energy, Oak Ridge, TN

☆U.S. GOVERNMENT PRINTING OFFICE 1989—648-119/00050